



UNIVERSITEIT•STELLENBOSCH•UNIVERSITY
jou kennisvennoot • your knowledge partner

Software-Defined Radio Based Pulse-Doppler Radar

C.A. van Zyl
20820127

Report submitted in partial fulfilment of the requirements of the module
Project (E) 448 for the degree Baccalaureus in Engineering in the Department of
Electrical and Electronic Engineering at Stellenbosch University.

Supervisor: Dr. J. Gilmore

November 2020

Acknowledgements

I would like to thank God the Father, the God of Abraham, Isaac and Jacob. Jesus Christ the Messiah, the Commander of the army of the Lord, and the Holy Spirit. Every breath I breathe is due to His grace and His grace alone. May this skripsi be for His glory and His glory alone.

Thank you Dr. Jacques Cilliers (CSIR) for the help you provided and the after-hour phone calls with screaming children in the background. Thank you Dr. Monique Potgieter (CSIR) for always encouraging me and being willing to help.

Thank you Dr. Jacki Gilmore for the supervision of this project and aiding in the difficulties of doing skripsi during a lockdown.

Thank you to my family. Without you, I would not have been able to spend these four years at university and work the long hours I did. Pa, Ma, Hendrik en Alèza ek is baie lief vir julle.

Thank you to all my friends for the support you have given me these 4 years. Alida, Jana, André, Raynhardt and Cullen, thank you for being good friends and making classes and long hours of work fun. Spesifiek die Pyntuin: Clint, Albertus, Heino en Janco ek is lief vir julle.

Thank you Erich Wiehahn for helping me with the statistical models of RCS fluctuation and how to implement them in software.



UNIVERSITEIT•STELLENBOSCH•UNIVERSITY
jou kennisvennoot • your knowledge partner

Plagiaatverklaring / Plagiarism Declaration

1. Plagiaat is die oorneem en gebruik van die idees, materiaal en ander intellektuele eiendom van ander persone asof dit jou eie werk is.

Plagiarism is the use of ideas, material and other intellectual property of another's work and to present it as my own.

2. Ek erken dat die pleeg van plagiaat 'n strafbare oortreding is aangesien dit 'n vorm van diefstal is.

I agree that plagiarism is a punishable offence because it constitutes theft.

3. Ek verstaan ook dat direkte vertalings plagiaat is.

I also understand that direct translations are plagiarism.

4. Dienooreenkomsdig is alle aanhalings en bydraes vanuit enige bron (ingesluit die internet) volledig verwys (erken). Ek erken dat die woordelikse aanhaal van teks sonder aanhalingstekens (selfs al word die bron volledig erken) plagiaat is.

Accordingly all quotations and contributions from any source whatsoever (including the internet) have been cited fully. I understand that the reproduction of text without quotation marks (even when the source is cited) is plagiarism

5. Ek verklaar dat die werk in hierdie skryfstuk vervat, behalwe waar anders aangedui, my eie oorspronklike werk is en dat ek dit nie vantevore in die geheel of gedeeltelik ingehandig het vir bepunting in hierdie module/werkstuk of 'n ander module/werkstuk nie.

I declare that the work contained in this assignment, except where otherwise stated, is my original work and that I have not previously (in its entirety or in part) submitted it for grading in this module/assignment or another module/assignment.

20820127 Studentenommer / Student number	 Handtekening / Signature
C.A. van Zyl Voorletters en van / Initials and surname	09/11/2020 Datum / Date

Abstract

English

This project investigates and develops an SDR based pulse-Doppler radar that is capable of measuring the range and velocity of vehicles. A statistical model of the radar range equation is developed to compare to the performance of the implemented radar. The hardware used includes an Ettus B210 SDR and two Ettus LP0965 antennas that collectively operate in the 850 MHz to 6 GHz range. The radar is designed to operate at 1.17 GHz since this provides a balance between SNR and foliage penetration. The radar is capable of detecting targets at 200, is small enough to be carried by one person and needs a new method of synchronisation when adding an amplifier, satisfying two of the three objectives. Future work involves real-time processing, foliage penetration, amplification and RCS characterization.

Afrikaans

Hierdie projek ondersoek en ontwikkel 'n SDR gebaseerde puls-Doppler radar wat die vermoëns het om die afstand en spoed van voertuie te meet. 'n Statistiese model van die radar-afstand vergelyking is ontwikkel om te vergelyk met die vermoëns van die geïmplementeerde radar. Die hardeware wat gebruik is sluit 'n Ettus B210 SDR en twee Ettus LP0965 antennas in wat gesamentlik in die 850 MHz tot 6 GHz reeks werk. Dit is ontwerp om teen 1.17 GHz te werk aangesien hierdie die beste balans tussen sein-tot-ruis en plantegroeipenetrasié bied. Dit kan voertuie op 200 m bespeur, is klein genoeg om deur een persoon gedra te word en kort 'n nuwe metode van sinkronisasie wanneer 'n versterker bygelas word, dus bevredig dit twee van die drie doele. Toekomstige werk sluit reëletydse verwerking, plantegroeipenetrasié, versterking en karakterisering van radar-deursnit in.

Contents

Declaration	ii
Abstract	iii
List of Figures	vii
List of Tables	ix
Nomenclature	x
1. Introduction	1
1.1. Background	1
1.2. Problem Statement	1
1.3. Project Objectives	1
1.4. Summary Of Work	2
1.5. Scope	2
1.6. Report Overview	2
2. Literature Study	3
2.1. Related Work	3
2.2. The Radar Equation	3
2.3. Pulsed Radar	5
2.4. The Doppler Effect	6
2.5. Matched Filter	7
2.6. Pulse Compression	9
3. System Overview	11
3.1. System Description	11
3.2. Software Defined Radio	12
3.3. Antennas	13
3.4. Software	14
3.4.1. GNU Radio	14
3.4.2. MatLab	14
3.4.3. UHD API	15
3.5. Summary	15

4. Radar Parameter Analysis	16
4.1. Power	16
4.2. Frequency	16
4.2.1. Antennas	17
4.2.2. Foliage Penetration	18
4.3. Pulse Repetition Frequency	19
4.4. Radar Cross-Section	20
4.5. Processing Gains	21
4.6. Thermal Noise	22
4.7. Losses	22
4.8. Clutter	23
4.9. The Radar Equation	23
4.10. Summary	24
5. System Implementation	25
5.1. Transmission	25
5.1.1. Block Diagram	25
5.1.2. Sample Rate	25
5.1.3. Gain	26
5.2. Reception	26
5.2.1. Block Diagram	26
5.2.2. Sample Rate	27
5.3. Transmission Signal	27
5.3.1. Transmission Length	27
5.3.2. Frequency Chirp	28
5.3.3. Pulse	28
5.4. Data Interface	29
5.4.1. Environment	29
5.4.2. Packets	30
5.4.3. Buffers	30
5.5. Processing	31
5.5.1. Synchronization	31
5.5.2. Pulse Compression	32
5.5.3. Doppler FFT	32
5.6. Resolution	33
5.7. Display	33
5.8. Mounting	34
5.9. Summary	34

6. Radar Performance	35
6.1. Basic Operation	35
6.2. Target Detection	36
7. Conclusion	38
7.1. Summary	38
7.2. Future Work	38
Bibliography	40
A. Project Planning Schedule	42
B. Exit Level Outcomes	43

List of Figures

2.1.	Basic operation of a pulsed radar.	5
2.2.	Range ambiguity that is caused in radars when the PRF is too high.	6
2.3.	Eclipsing that is caused when the radar cannot transmit and receive at the same time.	6
2.4.	The change in distance the signal travels due to the fact that the target is moving.	7
2.5.	The periodic nature of the phase shift caused by the Doppler effect.	7
2.6.	Model of a signal that is corrupted with additive Gaussian noise.	8
3.1.	High level system diagram of the radar.	11
3.2.	The SDR's that are available to loan from the CSIR.	13
3.3.	The antennas that are available to loan from the CSIR.	13
3.4.	Performance of the MatLab data interface between the host and the SDR, at different sampling frequencies.	15
4.1.	The setup used in the anechoic chamber when the pattern of the antennas was measured.	17
4.2.	The results from the measurements taken from the LP0965 antenna.	17
4.3.	Foliage attenuation models for electromagnetic signals.	18
4.4.	Setup and results from the RCS mean calculation.	20
4.5.	Swerling III RCS fluctuation models and the statistical manipulation.	21
4.6.	Radar detection range model with RCS fluctuation.	24
5.1.	The transmission block diagram of the system.	25
5.2.	Comparison of different gain values for the B210 transmission block.	26
5.3.	The reception block diagram of the system.	26
5.4.	The effect that windowing has on the maximum bandwidth of signals.	28
5.5.	The transmission signal pulse with zeros.	29
5.6.	The effect that packets and underflow has on phase.	30
5.7.	The thread diagram for the software in the data interface.	31
5.8.	Correlation of the packet received by the SDR to synchronize the transmission and reception.	31
5.9.	The effect of pulse compression on the transmission signal. Both signals are normalised to highlight the effect.	32

5.10. The FFT matrix used to calculate the Doppler frequencies.	32
5.11. The effect that the amount of pulses used in the Doppler FFT has on the velocity resolution. The received pulse was delayed to highlight the effect of the changes.	34
5.12. Mounting of the SDR and the antennas onto a plank of wood.	34
6.1. Measurements verifying the basic operation of the radar.	35
6.2. The road where the radar was tested.	36
6.3. Radar detecting two vehicles, one at 65 m and another at 150 m.	36
6.4. Detection of targets even though the clutter's amplitude is higher than that of the targets. The clutter is at a velocity of 0 m/s and the targets at a velocity of 12.24 m/s.	37
6.5. The radar detecting targets in the road by calculating the SNR instead of using the amplitude.	37

List of Tables

3.1. The specifications of the host system.	12
3.2. A comparison of the SDR's provided by the CSIR.	12
3.3. A comparison of the antennas provided by the CSIR.	13
A.1. Project planning schedule.	42
B.1. Exit level outcomes: descriptions and chapters.	43
B.2. Exit level outcomes: motivations.	44

Nomenclature

Acronyms and abbreviations

SDR	Software-Defined Radio
RADAR	RAdio Detection And Ranging
SNR	Signal-to-Noise Ratio
RCS	Radar Cross-Section
PDR	Pulse-Doppler Radar
USRP	Universal Software Radio Peripheral
LIDAR	Light Detection And Ranging
PRI	Pulse Repetition Interval
PRF	Pulse Repetition Frequency
FFT	Fast Fourier Transform
CSIR	Council for Scientific and Industrial Research
SMA	SubMiniature version A
USB	Universal Serial Bus
PC	Personal Computer
CPU	Central Processing Unit
RAM	Random Access Memory
GPU	Graphics Processing Unit
API	Application Programming Interface
UHD	USRP Hardware Driver
RF	Radio Frequency
PDF	Probability Density Function
DAC	Digital-to-Analogue Converter
ADC	Analogue-to-Digital Converter
DSP	Digital Signal Processing
ICASA	Independent Communications Authority of South Africa

Units

Hz	Hertz
kHz	Kilohertz
MHz	Megahertz
GHz	Gigahertz
m	Meters
mm	Millimeters
km	Kilometers
W	Watts
mW	Milliwatts
GB	Gigabytes
MSps	Megasamples per second
dB	Decibels
dBi	Decibels isotropic
dBsm	Decibels square meter
dBm	Decibels milliwatts
ppm	Parts per million
s	seconds
μ s	Microseconds
ns	Nanoseconds
m/s	Meters per second
km/h	Kilometers per hour
K	Kelvin
J/K	Joules per Kelvin
$^{\circ}$	Degrees

Chapter 1

Introduction

1.1. Background

The ability to see at long ranges and during bad weather conditions is a very useful capability for both civilian and military applications. Various methods have been used, starting at primitive binoculars, using balloons that were later replaced by aircraft [1] and later complex RAdio Detection And Ranging (RADAR) systems. Radars can be used for various applications including warfare, security, research and transportation.

The first leap towards radar technology happened in the 1880s when Heinrich Hertz verified the reflection of electromagnetic waves from objects [2]. This is the most important and fundamental concept that is necessary for radars to work. During this time until World War II there was not enough economic support to develop these kinds of systems and the first radars were only developed in the 1930s to be used in World War II [2]. Early radar systems did not have the performance that they have today since the technology and mathematics were not particularly developed.

1.2. Problem Statement

The technology used and developed in this project has various possible problems that it can solve. These two applications of radar will be investigated in this project:

1. Border control, specifically for cars being stolen and transported over the border to Mozambique.
2. A portable platform that can be used as a cost-effective research and development platform for radar is required.

1.3. Project Objectives

For the system to be a solution to the problems in the previous section, the objectives below have to be achieved.

1. Develop an initial radar system that can detect vehicles and measure their speed at 200 m.

2. Develop a radar system that is portable enough to be carried by one person.
3. The radar should be designed in such a way that an amplifier can be added without the need to change anything.

The rest of the report investigates and develops a system that achieves these objectives.

1.4. Summary Of Work

In this project, a full model of the radar performance is developed. The radar range equation is used to calculate the Signal-to-Noise Ratio (SNR) of the reflected signal at various distances. It is then used to compare to the actual system to see if the radar is performing as expected. The model includes the power received from a target, noise in the system, losses, processing gains and Radar Cross-Section (RCS) fluctuation. Furthermore, a Pulse-Doppler Radar (PDR) is developed that is capable of detecting vehicles and measuring their speed at 200 m. This is achieved by using an Ettus B210 and two Ettus LP0965 antennas that operate at 1.17 GHz and is small enough to be carried by one person.

1.5. Scope

The project focuses on the core concepts of radar systems and will lead to an understanding of the fundamentals. Some aspects are therefore not necessary to be implemented. A mounting system will not be developed for the radar since this focuses more on mechanical design. The radar will therefore not have a 360-degree field of view and will remain stationary. The radar will not be developed with an amplifier, since this is more expensive and can be added later on. It is therefore not necessary to be able to detect targets as far as might be required from problem statement 1 and a radar that can detect vehicles at 200 m is sufficient. The system can be upgraded in the future to perform real-time processing.

1.6. Report Overview

Chapter 1 is an introduction to the project and defines the problem statement and objectives. Chapter 2 explains the theory that is required to understand the content of this project and covers some theory and design that is not taught in undergraduate studies. Chapter 3 gives an overview of the system and the hardware used. Chapter 4 discusses the radar parameters and shows how each one is calculated. Chapter 5 discusses how the system is implemented from the antennas to the SDR to the host system. Chapter 6 gives the practical results and verifies that the system is working. Chapter 7 provides a summary and conclusion.

Chapter 2

Literature Study

2.1. Related Work

An SDR is a communications system that uses components implemented in software instead of hardware. This allows the user to change the design of the system without having to change the hardware. SDR's have been in use for more than 20 years and in this time it has been used in various applications, including radar related work. This section discusses these use cases.

S. Heunis, Y. Paichard and M. Inggs developed a prototype passive radar using the Universal Software Radio Peripheral (USRP) hardware platform along with the open-source GNU Radio SDR software [3]. They were able to detect commercial passenger aircraft at short ranges. They concluded that future work involves the designing of better receivers and implementing signal processing algorithms in real-time.

F. Peyrin and J.M. Friedt studied the abilities of SDR's as a passive radar to detect aircraft and allow safe operation of Light Detection And Ranging (LIDAR) [4]. They were able to detect aircraft at a distance of up to 5 km, flying 10 km above the lidar. They noted that their main constraint was the processing time of the signals.

R.G.L. de Mello, F.R. de Sousa and C. Junqueira introduced an SDR-based radar-detector and how it can be used on a low power device [5]. They were able to accurately measure pulses in real-time on a low power tablet.

From the work related to this project, it is clear that developing a PDR on an SDR is viable.

2.2. The Radar Equation

The radar equation is the core concept used in estimating and assessing the performance of the radar. It uses the transmission power, received power and power of the noise to calculate the SNR of the targets sensed by the system and thus the maximum range at which it can operate. It begins by calculating the power density on the surface of a sphere with

$$P_{\text{sphere}} = \frac{P_{\text{pk}}}{4\pi R^2} \quad \text{watts/m}^2 \quad (2.1)$$

where P_{sphere} is the power on the surface of the sphere, P_{pk} is the peak power of the transmitted signal and R is the distance from the antenna. The power density due to the use of a directive antenna can be calculated by

$$P_{\text{ant}} = \frac{P_{\text{pk}}G_{\text{ant}}}{4\pi R^2} \quad \text{watts/m}^2 \quad (2.2)$$

where G_{ant} is the directive gain from the antenna. The signal will impinge on a target and reflect back. The amount of signal reflected depends on the RCS of the target. The RCS is "the measure of a target's ability to reflect radar signals in the direction of the radar receiver, i.e. it is a measure of the ratio of backscatter density in the direction of the radar (from the target) to the power density that is intercepted by the target" [6]. The power incident on the target is calculated by

$$P_{\text{target}} = \frac{P_{\text{pk}}G_{\text{ant}}\sigma}{4\pi R^2} \quad \text{watts} \quad (2.3)$$

where σ is the RCS of the target. The target can be seen as another transmitter that scatters spherically. Thus the power received can be calculated by

$$P_{\text{rec}} = \frac{P_{\text{pk}}G_{\text{ant}}\sigma}{4\pi R^2} \times \frac{A_e}{4\pi R^2} = \frac{P_{\text{pk}}G_{\text{ant}}A_e\sigma}{(4\pi)^2 R^4} \quad \text{watts} \quad (2.4)$$

where A_e is the effective area of the antenna. The gain of the antenna is calculated from $G_{\text{ant}} = \frac{4\pi A_e}{\lambda^2}$. And thus, $A_e = \frac{G_{\text{ant}}\lambda^2}{4\pi}$. Substituting this into equation 2.4 gives

$$P_{\text{rec}} = \frac{P_{\text{pk}}G_{\text{ant}}^2\lambda^2\sigma}{(4\pi)^3 R^4} \quad \text{watts.} \quad (2.5)$$

The SNR can now be calculated by taking the power of the noise, losses and processing gains into account with

$$\text{SNR} = \frac{P_{\text{pk}}G_{\text{ant}}^2\lambda^2\sigma G_p}{(4\pi)^3 R^4 P_n L_{\text{tot}}} \quad (2.6)$$

where P_n is the power of the noise, L_{tot} represents the total losses in the system and G_p is the combination of all the processing gains in the system.

This is the basic equation that is used in the analysis of radar performance. However, each of the elements can become extremely complicated and can be studied in its own right. This is outside the scope of the project and the equation is sufficient as is.

2.3. Pulsed Radar

Pulsed radar exploits the principle that electromagnetic waves reflect off objects. This reflected signal is then received by the radar and can be seen in Fig. 2.1. The Pulse Repetition Interval (PRI) is the period of the pulses and $\text{PRI} = \text{PRF}^{-1}$ where PRF is the Pulse Repetition Frequency. The time it takes for the echo to be received can be used to calculate the distance of the target. Since the electromagnetic wave travels at the speed of light and needs to travel to the target and back, the distance can be calculated by

$$R = \frac{\tau c}{2} \quad [7] \quad (2.7)$$

where R is the distance of the target, c is the speed of light and τ is the time taken for the echo to be detected, as seen in Fig. 2.1.

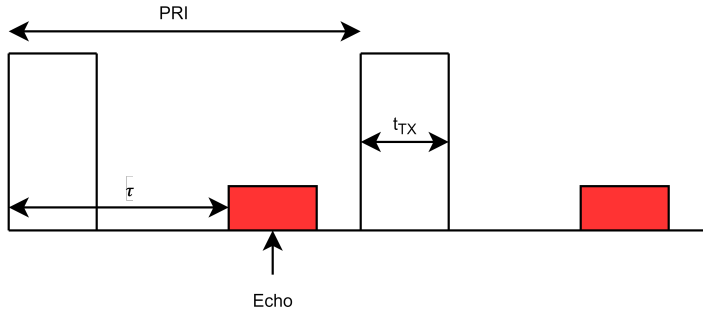


Figure 2.1: Basic operation of a pulsed radar.

An aspect of pulsed radars to take into account when designing is the possibility of range ambiguity. When the PRF is too high, another pulse can be transmitted before the echo from the first one is received as can be seen in Fig. 2.2. It can be avoided by designing the radar so that it does not detect targets further than the PRF allows, or by allowing for ambiguity and using signal processing to resolve it. The first solution is simpler and within scope. The maximum range can be calculated by

$$R_{\max} = \frac{(\text{PRI} - t_{\text{TX}}) \times c}{2} \quad (2.8)$$

where R_{\max} is the maximum range the radar should be able to sense a target and t_{TX} is the transmission time of the system as seen in Fig. 2.2.

With high power radars reception has to be disabled while it is transmitting to prevent the radar receiver from being damaged. This means that while the radar is transmitting, there can be no received signals (the radar is completely blind) or only partially received signals (eclipsing). Eclipsing can be seen in Fig. 2.3. The blind range (or dead zone) can be calculated by

$$R_{DZ} = \frac{t_{TX} \times c}{2} \quad (2.9)$$

where R_{DZ} is the blind range (where the radar cannot sense or can only sense partially) and t_{TX} is the transmission time, as seen in Fig. 2.3.

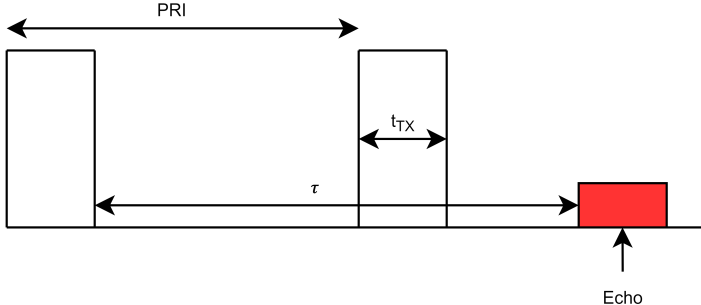


Figure 2.2: Range ambiguity that is caused in radars when the PRF is too high.

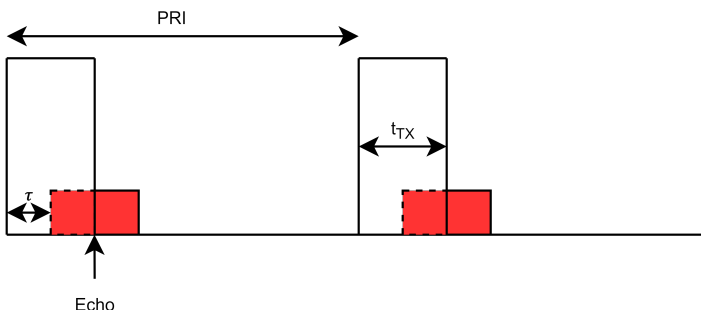


Figure 2.3: Eclipsing that is caused when the radar cannot transmit and receive at the same time.

2.4. The Doppler Effect

The Doppler effect occurs when a moving target reflects the signal, but with a change in frequency that leads to a change in phase for radars, as seen in Fig. 2.4 and 2.5 [7]. This effect can also occur when the observer is in motion. The change in frequency (or change in distance travelled which leads to a change in phase) can then be used to calculate the relative velocity of the target. The relative velocity can be calculated by

$$V_r = \frac{d}{\text{PRI}} = d \times \text{PRF} \quad (2.10)$$

where V_r is the relative velocity and d is the distance as seen in Fig. 2.4 [7]. Since the radar is stationary, the relative velocity, V_r , is the velocity of the target. This difference in phase can be calculated by

$$\Delta\phi = 2d \frac{2\pi}{\lambda} \quad (2.11)$$

where $\Delta\phi$ is the phase change. Since the change in phase occurred over one PRI, the rate of change can be calculated by

$$\omega_d = \Delta\phi \times \text{PRF} = \frac{2d2\pi \times \text{PRF}}{\lambda} \quad (2.12)$$

and thus the Doppler frequency can be calculated by

$$f_d = \frac{\omega_d}{2\pi} = \frac{2d \times \text{PRF}}{\lambda}. \quad (2.13)$$

By substituting in equation 2.10 one obtains

$$f_d = \frac{2V_r}{\lambda}. \quad (2.14)$$

The Doppler frequency can be calculated by using a Fast Fourier Transform (FFT) on the received signals, and thus, the velocity of the target can be calculated by

$$V_r = \frac{f_d \lambda}{2}. \quad (2.15)$$

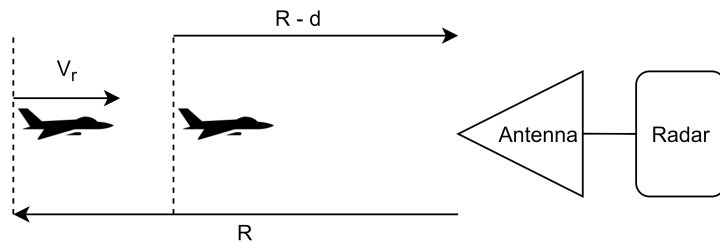


Figure 2.4: The change in distance the signal travels due to the fact that the target is moving.



Figure 2.5: The periodic nature of the phase shift caused by the Doppler effect.

2.5. Matched Filter

A matched filter is the optimum linear filter for maximizing the SNR when the system is corrupted by additive Gaussian noise. Fig. 2.6 shows a model of a signal that is corrupted

by additive Gaussian noise [7].

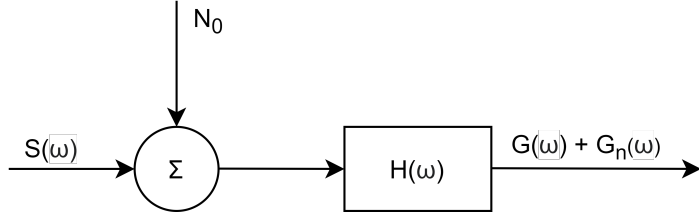


Figure 2.6: Model of a signal that is corrupted with additive Gaussian noise.

From Fig. 2.6 the output signal is

$$G(\omega) = S(\omega)H(\omega), \quad (2.16)$$

which can be written in the time domain as

$$g(t) = \frac{1}{2\pi} \int_{-\infty}^{+\infty} S(\omega)H(\omega)e^{j\omega t} d\omega. \quad (2.17)$$

The noise power can be calculated by

$$G_n(\omega) = \frac{N_0}{2}|H(\omega)|^2, \quad (2.18)$$

and the mean can be calculated by

$$\sigma_n^2 = \left(\frac{1}{2\pi} \right)^2 \int_{-\infty}^{+\infty} \frac{N_0}{2} |H(\omega)|^2 d\omega. \quad (2.19)$$

By integrating over all the frequencies, the SNR can be calculated by

$$\text{SNR} = \frac{g^2(t)}{\sigma_n^2} = \frac{\left| \int_{-\infty}^{+\infty} S(\omega)H(\omega)e^{j\omega t} d\omega \right|^2}{\frac{N_0}{2} \int_{-\infty}^{+\infty} |H(\omega)|^2 d\omega}. \quad (2.20)$$

$H(\omega)$ has to be found so that the expression is maximized and the Cauchy-Schwartz inequality can be used [7]. It states that the inner product has a maximum value when the two vectors are aligned and is given by

$$\left| \int f(x)g(x)dx \right|^2 \leq \int |f(x)|^2 dx \int |g(x)|^2 dx. \quad (2.21)$$

Thus the SNR is a maximum when

$$\left| \int S(\omega)H(\omega)d\omega \right|^2 = \int |S(\omega)|^2 dx \int |H(\omega)|^2 dx. \quad (2.22)$$

This can be rewritten as

$$H(\omega) = kS^*(\omega)e^{-j\omega t'} \quad (2.23)$$

where k is a scaling factor and t' is a phase shift factor. Equation 2.23 is the matched filter.

2.6. Pulse Compression

Pulse compression is a specific form of matched filtering that allows the designer the freedom to decouple the pulse length of a radar from the resolution. An increased resolution allows the radar to detect targets that are closer to each other. The range resolution of an uncoded pulse is given by t_{TX} , but with pulse compression it is given by $\frac{c}{2 \times B}$ [7]. Firstly, the correlation of two functions is given by

$$r_{xy}(t') = \lim_{T_0 \rightarrow \infty} \frac{1}{T_0} \int_{-\frac{T_0}{2}}^{+\frac{T_0}{2}} f_1(t)f_2(t+t')dt \quad [7] \quad (2.24)$$

where t' represents a time shift and T_0 is the correlation period. Since the signals are limited, it is better to use the finite version of the correlation function that is given by

$$r_{xy}(t') = \int_{-\infty}^{+\infty} f_1(t)f_2(t+t')dt. \quad (2.25)$$

If one correlates the same signal, it turns into the autocorrelation function that is given by

$$r_{xx}(t') = \int_{-\infty}^{+\infty} f(t)f(t+t')dt. \quad (2.26)$$

Assuming the radar function returns a signal $S(\omega)$ and is processed by a receiver that has a transfer function $H(\omega)$,

$$G(s) = S(\omega)H(\omega), \quad (2.27)$$

which can be represented in the time domain as

$$g(t) = \int_{-\infty}^{+\infty} s(t')h(t-t')d\tau. \quad (2.28)$$

It is clear that equations 2.26 and 2.28 are very similar and the only significant difference is the convolution integral. For the receiver to be matched to the received signal, it must

be the complex conjugate of the signal and is given by

$$H(\omega) = S^*(\omega), \quad (2.29)$$

then

$$G(s) = S(\omega)S^*(\omega), \quad (2.30)$$

which can be written in the time domain as

$$g(t) = \int_{-\infty}^{+\infty} s(t')s(t+t')d\tau. \quad (2.31)$$

This receiver leads to a gain in SNR of

$$G_{SNR} = \frac{t_{TX}}{\frac{1}{B}} = t_{TX}B \quad (2.32)$$

where t_{TX} is the transmitted pulse width and B is the compressed pulse bandwidth.

Chapter 3

System Overview

This section discusses the high-level design decisions that were made and gives an overview of the system operation. The project scope is largely determined by the budget and the options for hardware were limited to what the CSIR [8] was able to loan to Stellenbosch University.

3.1. System Description

The system consists of three basic components: the antennas, the SDR and the host system. This can be seen in Fig. 3.1. The antennas and SDR are connected with SubMiniature version A (SMA) cables and the SDR is connected to the host system via Universal Serial Bus (USB) cables.

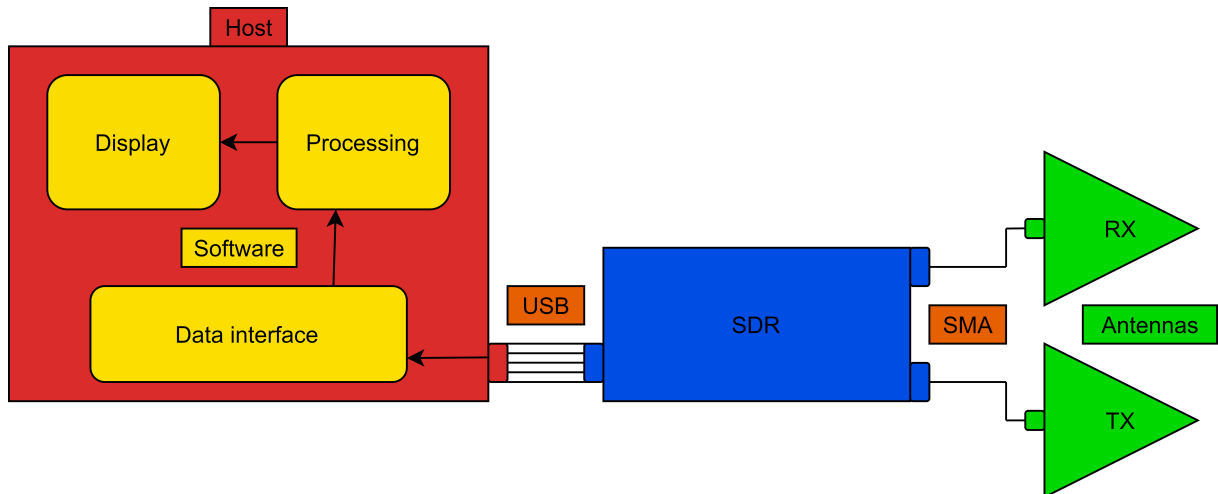


Figure 3.1: High level system diagram of the radar.

The host is where the processing and display of the system take place. This can be any laptop or Personal Computer (PC), but depending on the performance of the host, the performance of the radar can be severely impacted. The specifications of the laptop used can be seen in Table 3.1. It has a powerful Central Processing Unit (CPU), enough Random Access Memory (RAM) and the USB connection is sufficient. However, a faster USB port would yield better results in terms of data rates.

Table 3.1: The specifications of the host system.

Metric	Wootbook Metal II
CPU	Ryzen 7 4800H 8C16T
GPU	Radeon RX Vega 7 Integrated
RAM	2×16GB DDR4 2400 MHz
Memory	1TB NVMe M.2
USB	Gen 3.1

3.2. Software Defined Radio

The SDR's on the market range from cheap entry-level products, to very expensive professional products. When choosing an SDR the limiting factor is the budget of the project. For the scope of this project, something as simple as the SDRplay RSPdx is too expensive, coming in at \$200.00 [9]. Although this SDR covers a wide range of frequency bands (1 kHz to 2 GHz), it lacks in terms of the sampling frequency, going up to 10.66 MSps [10]. This would be sufficient to develop a radar system, however, the performance and resolution would be lacking compared to the other options available. The CSIR was able to provide the Ettus B210 (Fig. 3.2a) [11] or the Nuand BladeRF 2.0 Micro (Fig. 3.2b) [12]. A comparison is drawn between these two SDR's and can be seen in Table 3.2.

Table 3.2: A comparison of the SDR's provided by the CSIR.

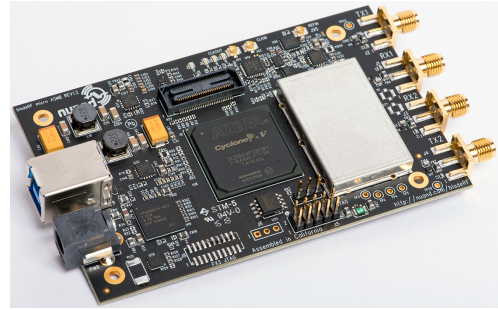
Metric	B210	BladeRF Micro 2.0
Company	Ettus	Nuand
Frequency range	70 MHz - 6 GHz	70 MHz - 6 GHz
Output power	10 mW	6.31 mW
Sampling rate	61.44 MSps	61.44 MSps
Noise figure	8 dB	-
ADC/DAC resolution	12 Bits	12 Bits
Frequency accuracy	±2.0 ppm	-

Another factor to consider, in addition to the specifications in the table, is the amount of documentation available. The B210 has detailed documentation on how to use the SDR and a full description of the Application Programming Interface (API) that is used

to communicate with the device [13]. The BladeRF, on the other hand, does not have sufficient documentation. This, along with the fact that the B210 has slightly better specifications, makes it the better choice for the radar.



(a) The Ettus B210.



(b) The Nuand BladeRF Micro 2.0.

Figure 3.2: The SDR's that are available to loan from the CSIR.

3.3. Antennas

Ettus has a variety of antennas that can be used with their SDR's, ranging from omnidirectional to directional log-periodic antennas [14]. The CSIR has two models that they are able to provide and a comparison can be seen in Table 3.3.

Table 3.3: A comparison of the antennas provided by the CSIR.

Metric	LP0965	LP0410
Frequency range	850 MHz - 6.5 GHz	400 MHz - 1 GHz
Size (B × H)	134 mm × 142 mm	260 mm × 290 mm
Gain	5 - 6 dBi	5 - 6 dBi
Type	Log periodic	Log periodic



(a) LP0965.



(b) LP0410.

Figure 3.3: The antennas that are available to loan from the CSIR.

From Table 3.3 it is clear that the LP0965 (Fig. 3.3a) is a smaller antenna and will be portable, but will not have the lower frequency capabilities that the LP0410 (Fig. 3.3b) has. Although the LP0410 can achieve lower frequencies, it is larger and less portable. For this project, portability is valued more than foliage penetration due to objective 2 and the smaller antenna is chosen. However, it can easily be swapped if needed.

3.4. Software

When deciding on a software interface for the radar system, there are 3 options to choose from: GNU Radio, MatLab and the USRP Hardware Driver (UHD) API.

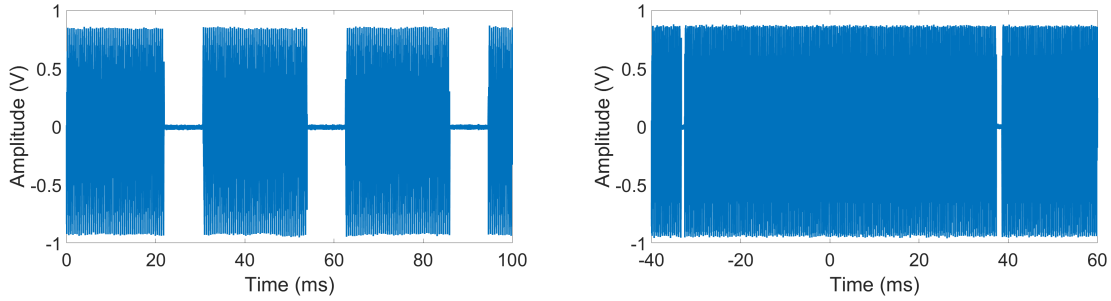
3.4.1. GNU Radio

GNU Radio is a python based, open-source development kit that provides signal processing software blocks that can be used to implement software radios [15]. It is very simple and easy to use, and implementing receive or transmission systems are very easy. However, radar systems are very demanding and to have one that performs well, the software must be able to handle very high data rates and be able to transmit and receive simultaneously. Although GNU radio might be able to achieve these requirements to some degree, it does not have a low-level interface that can communicate with the SDR. Thus, GNU Radio is dismissed for one of the other options.

3.4.2. MatLab

Another option that is considered is MatLab. There are two possible options when considering MatLab - using Simulink or the USRP support package [16]. Simulink is very similar to GNU Radio since it also implements the signal processing via software blocks and is dismissed for the same reasons. However, the USRP support package is created specifically for Ettus products and allows some form of lower-level programming and might be sufficient. This software package is tested to see how well it performs and the results can be seen in Fig. 3.4.

From Fig. 3.4 it is clear that the MatLab toolbox is not capable of handling the high data rates required for the system and the host cannot keep up with the data requested from the SDR. In addition to this, it does not perform well enough to be able to transmit and receive simultaneously. For these reasons, MatLab is dismissed as the data interface. However, MatLab has good and easy to use mathematical and display functions and will be used for post-processing.



(a) SDR transmission with MatLab at a sampling frequency of 16 MSps. **(b)** SDR transmission with MatLab at a sampling frequency of 5.33 MSps.

Figure 3.4: Performance of the MatLab data interface between the host and the SDR, at different sampling frequencies.

3.4.3. UHD API

Ettus provides a low-level API that can be used to communicate with their line of SDR's - the UHD API [13] and is available in C++ and Python. Since performance is crucial for this system, C++ is chosen. C++ can be compiled and executed, allowing it to run faster than Python, which is a scripting language. Writing display and processing functions are more difficult in C++, thus MatLab will be used.

3.5. Summary

This chapter investigated the possible hardware and software available for the system. The choices were limited to the budget and the hardware components used are on loan from the CSIR. The components used are:

- SDR - Ettus B210.
- Antennas - Ettus LP0965.
- Data interface - Ettus UHD API.
- Post-processing - MatLab.

The implementation of these components can be seen in chapter 5.

Chapter 4

Radar Parameter Analysis

This section discusses the choice of parameters and some of the design decisions of the radar. These decisions and parameters are used to develop a model of the radar's performance and will help highlight the effect that changes in parameters have on the system. This model will also be used as a comparison to see if the physical system performs as expected. Refer to Fig. 4.6 for the final model.

4.1. Power

Power is a limiting factor for the system. The Ettus B210 draws its power via a USB connection from a laptop or PC. This means that the transmission power of the radar is low and according to the datasheet it has a maximum of 10 mW [17]. The low power can be addressed by using an amplifier that can turn off in the reception period, but this is beyond the scope of this project. If the final model is capable of sensing targets at the required distance, the power levels will be sufficient. This can be seen in Fig. 4.6.

4.2. Frequency

The transmitted signal of the radar has to be modulated onto a carrier signal. This signal has to be chosen carefully since it can influence the performance of the radar by reducing the SNR or causing interference from other Radio Frequency (RF) sources.

The first and most obvious limitations to the decision are the capabilities of the chosen hardware. The Ettus B210 has a frequency range of 70 MHz to 6 GHz [11] and the antennas used have a range of 850 MHz to 6.5 GHz [18]. Thus, the frequency must be chosen in the range of 850 MHz to 6 GHz.

The second factor to take into account when choosing a frequency is looking at the frequencies available from the Independent Communications Authority of South Africa (ICASA) table [19]. To minimize interference from other sources and transmit legally, a frequency that is not in use is chosen. The chosen frequency is discussed in the following sections.

4.2.1. Antennas

According to the datasheet, the antennas have a typical forward gain of 6 dBi [18]. To evaluate which frequencies will yield the best performance from the antenna, two measurements are made - the S11 parameter and the beam pattern. The S11 parameter describes how much of the signal is reflected from the antenna and a lower value is desired. The beam pattern shows the antenna gain as a function of angle and a smooth pattern is desired. The beam patterns were measured in an anechoic chamber and can be seen in Fig. 4.1. The S11 parameters were measured using a vector network analyzer (the Agilent Technologies PNA-X Network Analyser, N5242A). The results of both these measurements can be seen in Fig. 4.4.



Figure 4.1: The setup used in the anechoic chamber when the pattern of the antennas was measured.

From Fig. 4.2a it is clear that the frequency with the best S11 value is 5.7728 GHz. However, from equation 2.6 it is clear that lower frequencies improve the SNR (due to the effect of the λ term) and a lower frequency point will also be compared. The lowest frequencies that still have low S11 values are at 1.1012 GHz and 1.1692 GHz. However, from Fig. 4.2b it is clear that the beam pattern at 1.18 GHz is more even and therefore a better choice.

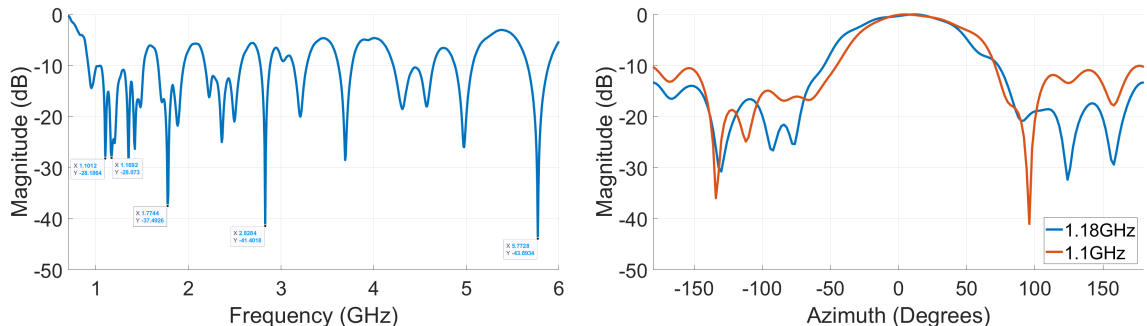


Figure 4.2: The results from the measurements taken from the LP0965 antenna.

The two chosen frequencies have to be compared to see which one yields the highest SNR. The SNR gain due to the λ term in equation 2.6 can be calculated by

$$G_f = 10\log(\lambda) = 10\log\left(\frac{c}{f_c}\right). \quad (4.1)$$

Therefore, $G_{1.17\text{GHz}} = -5.91$ dB and $G_{5.77\text{GHz}} = -12.84$ dB. Now the S11 parameter has to be taken into account. If 5.77 GHz is taken as the reference point, 43.89 dB – 28.07 dB = 15.82 dB should be subtracted from $G_{1.17\text{GHz}}$, leading to a value of -5.91 dB – 15.82 dB = -21.73 dB. It is clear that the higher frequency leads to a higher SNR. However, there is one more aspect to take into consideration.

4.2.2. Foliage Penetration

Foliage penetration is the ability of electromagnetic waves to penetrate foliage. The Weissberger (optimistic) models are given by [20]

$$L = 0.45f^{0.284}d \quad (0m < d < 14m), \quad (4.2)$$

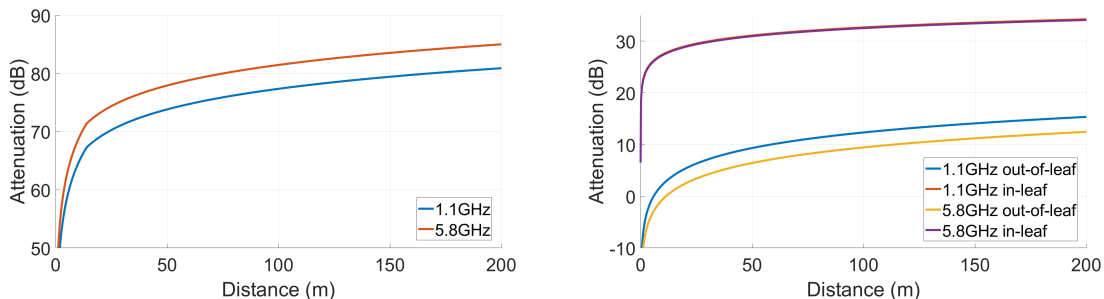
$$L = 1.33f^{0.284}d^{0.588} \quad (14m < d < 400m), \quad (4.3)$$

where L is attenuation, f is the frequency of the carrier and d is the tree depth in meters. The FITUR (pessimistic) models are given by [20]

$$L = 26.6f^{-0.2}d^{0.5} \quad (\text{out-of-leaf}), \quad (4.4)$$

$$L = 15.6f^{-0.009}d^{0.26} \quad (\text{in-leaf}), \quad (4.5)$$

where L is attenuation, f is the frequency of the carrier and d is the tree depth in meters.



(a) The Weissenberger foliage attenuation model (b) The FITUR foliage attenuation model at different frequencies.

Figure 4.3: Foliage attenuation models for electromagnetic signals.

The performance at different frequencies can be seen in Fig. 4.3. From these models, it is

clear that lower frequencies penetrate foliage better. The lower 1.17 GHz is, therefore, a better option than 5.77 GHz, since it will allow the radar to penetrate foliage better in scenarios where foliage is in the way of targets.

4.3. Pulse Repetition Frequency

The PRF describes the rate at which the pulses are transmitted from the radar. It has to be chosen to be as high as possible since this will allow the system to integrate received signals in the shortest amount of time. The higher the PRF for a fixed pulse length, the higher the SNR. However, it should not be so high that it causes range ambiguity. This occurs when the system receives a return in pulse N+1 (N+2, N+3, ...) that belongs to pulse N. It can be prevented by taking it into account when choosing the PRF. If a maximum measurable distance is to be taken as 1 km (to satisfy objective 1 when an amplifier is added), the maximum PRF is calculated in equations 4.6 to 4.8.

$$R = \frac{c \times \tau}{2} \quad (4.6)$$

$$\tau = \frac{2 \times R}{c} = 6.67 \mu\text{s} \quad (4.7)$$

$$\text{PRF} = \tau^{-1} \approx 150 \text{ kHz} \quad (4.8)$$

Where c is the speed of light and τ is the time taken for the target to be detected by the radar [7]. It is thus clear that to prevent ambiguity, the maximum PRF is 150 kHz. This value can be changed if the radar performs worse or better than expected.

One must also consider the possibility of Doppler ambiguities. To prevent this, the sampling frequency (in the case of Doppler processing, this is the PRF) must be twice that of the highest frequency sampled [7]. The maximum frequency that can be samples (and thus the highest velocity measurable) is calculated by

$$f_{\max} = 0.5 \times \text{PRF} = 75 \text{ kHz.} \quad (4.9)$$

The maximum velocity measurable is calculated by [7]

$$V_r = \frac{f_d \times \lambda}{2} = \frac{f_d \times c}{2 \times f_c} = 9,608.73 \text{ m/s} \quad (4.10)$$

where f_d is the Doppler frequency and f_c is the carrier frequency. From equation 5.7 it is clear that Doppler ambiguity will not be a problem with the chosen PRF for the targets of interest.

4.4. Radar Cross-Section

No design decisions have to be made regarding the RCS itself, but a model of the RCS is used to help simulate the radar performance. The Swerling models [7] of RCS that are used in the simulation is given by

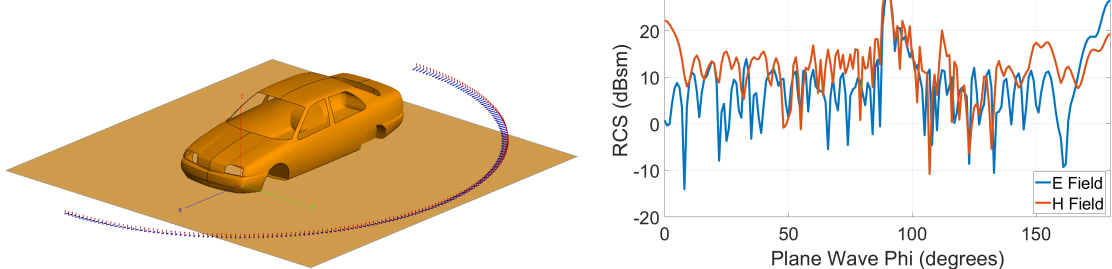
$$w(x, \bar{x}) = \frac{1}{\bar{x}} \exp\left(\frac{-x}{\bar{x}}\right) \quad (x \geq 0), \quad (4.11)$$

$$w(x, \bar{x}) = \frac{4x}{\bar{x}^2} \exp\left(\frac{-2x}{\bar{x}}\right) \quad (x \geq 0), \quad (4.12)$$

where \bar{x} is the mean of the RCS, equation 4.11 describes cases I and II and equation 4.12 describes cases III and IV. Cases I and III describes scan-to-scan variation and cases II and IV describes pulse-to-pulse variation. To choose a model, one must first determine if the RCS will change from scan-to-scan or pulse-to-pulse. From the PRF of 150 kHz, the pulses will be $150,000^{-1} = 6.67 \mu\text{s}$ apart. If a relatively average speed of 120 km/h is taken for a vehicle, it will be able to travel $120/3.6 \times 6.67 \mu\text{s} = 0.222 \text{ mm}$ between pulses. Civilian vehicles also have very slow rotational speeds. It is thus clear that it will not have pulse-to-pulse variation.

Next, the decision between cases I and III has to be made. The differences between cases I and III are the reflective areas of the objects. For case I, "Assumes that the target consists of a random assembly of scatterers, all equally weighted" [7] and for case III, "Assumes that the target consists of one dominant reflector plus several small sub reflectors" [7]. It is thus clear that case III will be the best model for civilian vehicles.

To implement these RCS models, the mean of the targets must first be calculated. Since RCS changes with frequency, it is necessary to simulate the RCS in FEKO to acquire a value for the specific application. The 3D model of a generic vehicle used can be seen in Fig. 4.4a. The RCS calculated by FEKO (from Fig. 4.4b) can be used to calculate the mean and is calculated as 7.97 dBsm. This value is used as \bar{x} in equations 4.11 and 4.12.



(a) 3D FEKO model of a generic vehicle used to **(b)** RCS calculations from FEKO for a generic calculate the mean RCS. vehicle at 1.17 GHz.

Figure 4.4: Setup and results from the RCS mean calculation.

To be able to model the variation of RCS in software, equations 4.11 and 4.12 have to

be used. However, these Probability Density Functions (PDF) cannot be implemented directly in MatLab and have to be manipulated. To be able to sample from the PDF, the inverse of the cumulative PDF must be calculated. This function can then be sampled via a uniform distribution, as seen in Fig. 4.5b. Refer to Fig. 4.6 for the implementation and use of the model.

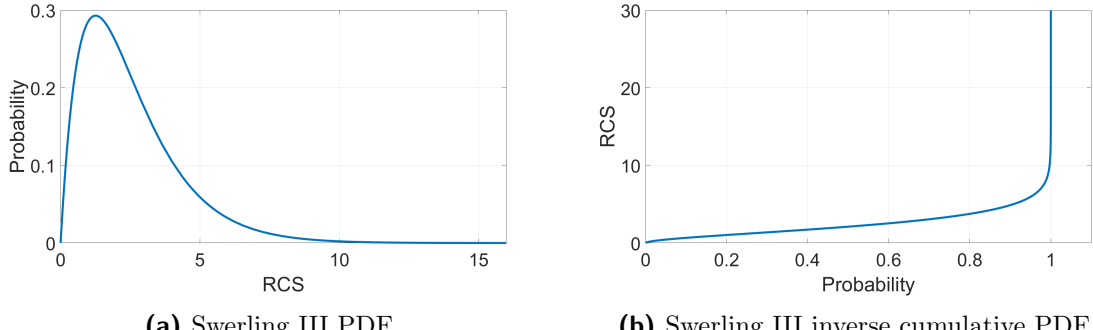


Figure 4.5: Swerling III RCS fluctuation models and the statistical manipulation.

4.5. Processing Gains

To increase the radar detection performance the SNR must be increased. This can be achieved by changing any of the parameters of the radar equation. However, for this project, the only adjustable parameters are the frequency and processing gains.

A processing technique used is pulse compression. This is used to increase the resolution of the system, but also provides a gain in SNR. This gain is given by [7]

$$G_{\text{SNR}} = t_{\text{TX}} B \quad (4.13)$$

where t_{TX} is the pulse length and B is the signal pulse duration. From section 5.3.2 the bandwidth is 7 MHz, from section 5.3.1 the transmission length is 13 samples and from section 5.1.2 the sampling frequency is 16 MHz. The transmission time can be calculated by $T_{\text{TX}} = f_s^{-1} \times 13 = 812.5\text{ns}$. This leads to a pulse compression gain of 7.55 dB.

The FFT is a crucial part of the radar system and is used in Doppler processing. When an FFT with a window is performed on a signal it improves the SNR and is given by [21]

$$G_{\text{SNR}} = \frac{\left(\sum_n w(nT) \right)^2}{\sum_n w^2(nT)} \quad (4.14)$$

where w is the window function used. From section 5.5.3 a Blackman window is used with $\text{PRF} \times 2 = 300,000$ samples since the radar is transmitting for two seconds. This leads to a gain in SNR of 52.40 dB.

4.6. Thermal Noise

Thermal noise is present in all electronic systems and cannot be removed or filtered out, since it covers the entire frequency spectrum. This is the largest limiter of radar performance since the received signal becomes smaller than the noise present at long distances. The minimum value can be calculated by

$$N_i = kTB_N \quad (4.15)$$

where $k = 1.38 \times 10^{-23}$ J/K, $T = T_0 = 290$ K and B_N is the noise bandwidth of 7 MHz [7]. This leads to $N_i = -135.53$ dB and is the absolute minimum value.

The noise is increased further by the amplification of the signal. The noise figure is described as "The factor by which the noise on the output of an ideal device must be increased to give the same noise level out of the actual device" [7] and is given by

$$F = \frac{\text{SNR}_i}{\text{SNR}_o} \quad (4.16)$$

where SNR_i is the input SNR (receiver) and SNR_o is the output SNR (transmitter). The Ettus B210 has a worst case noise figure of 8 dB [17]. Thus, the noise in the system becomes -135.53 dB + 8 dB = -127.53 dB.

4.7. Losses

In addition to the noise present in the system, some factors cause the signal to lose power or noise to increase and reduce the SNR.

The transmission signal will be a sampled signal and the bandwidth must be half the sampling frequency, according to Nyquist's theory. The signal will also be finite (multiplied by a square window function). This means that the frequency domain of the square window (a sinc function) will have large sidelobes and cause aliasing. To minimize this effect, a Blackman window is applied. This leads to a worst-case SNR loss of 3.29 dB [21]. Other windows have smaller SNR reductions, but the sidelobe reductions are not as good as the Blackman window's. Refer to Fig. 5.4 for the use of the window.

When a signal is being transmitted, it goes through the DSP chain and RF frontends. This process will lead to a small loss of 1 dB [22].

Electromagnetic waves also undergo attenuation since they are being transmitted through the atmosphere. However, for a radar that operates under 3 GHz, this loss is negligible [22].

4.8. Clutter

Clutter is the reflections that are received from targets that are not of interest. There are different types of clutter, and therefore different equations to describe each of them. The applicable models are discussed in this section.

The first model is an area with a large number of equally weighted independent scatterers. From [7], "It is appropriate to wooded land at grazing angles $> 5^\circ$, sea clutter over large-resolution cells, sea clutter over small-resolution cells at a grazing angle $> 5^\circ$, as well as rain clutter and chaff." This model is known as the Gaussian (Rayleigh) model and is given by

$$p(\sigma^\circ) = \frac{1}{\sigma_0^\circ} \exp\left(-\frac{\sigma^\circ}{\sigma_0^\circ}\right) \quad (4.17)$$

where σ_0° is the standard deviation in the backscatter coefficient, σ° .

The next model to study is the Rician model. From [7], "Rician clutter is applicable in circumstances where there are many independent scatterers plus a dominant steady component that may typically arise from tree trunks, pylons, buildings, or rocks. It is also a good representation of the temporal characteristics of land clutter." This model is given by

$$p(\sigma^\circ) = p(P) = \frac{1 + m^2}{P_s + P_v} \exp(-m^2) \exp\left(-\frac{P(1 + m^2)}{P_s + P_v}\right) I_0\left(2m\sqrt{\frac{P(1 + m^2)}{P_s + P_v}}\right) \quad (4.18)$$

where

$$m^2 = \frac{P_s}{P_v} \quad (4.19)$$

where P_s is the steady power and P_v is the mean variable power. Clutter is an important concept and is included for the sake of comprehensiveness. When implementing the Doppler FFT on the received signals, stationary targets (including clutter) are separated from moving targets. Thus, the radar will not be clutter limited, but noise limited.

4.9. The Radar Equation

All of the parameters discussed in this chapter are combined to form a model of the radar performance using the radar range equation, from equation 2.6. An SNR threshold of 15 dB is chosen. The 89dB that is available from the Ettus B210 transmission hardware is not included in the SNR equation, since this increases both the signal and the noise. The final radar equation is given by

$$\text{SNR} = \frac{G_{\text{ant}}^2 \times E_{\text{pulse}} \times \sigma \times \lambda^2 \times PC_{\text{gain}} \times FFT_{\text{gain}}}{R^4 \times (4\pi)^3 \times L_{\text{tot}} \times P_{\text{noise}}} \quad (4.20)$$

where E_{pulse} is the energy of a single pulse.

In high power radars, the receive port is disabled while the radar is transmitting. It is disabled due to the high power output of the transmission. This causes the radar to have a dead zone, an area where the radar is blind. The blind range is dependant on the transmission time and can be calculated as seen in equation 2.9.

A possible solution to this problem is to transmit two different pulses - one to detect long-range targets and another shorter pulse to detect close-range targets. This is also implemented in the model to keep the possibility of adding an amplifier open. The blind range of the short-range pulse is the area where the radar is completely blind, so this value has to be chosen. A distance of 50 m is chosen as an acceptable blind range. From this, the maximum range at which the radar can detect is 140 m and the blind range of the long-range pulse is chosen as 120 m. This allows the radar to detect targets at a greater distance than 200 m and therefore satisfies objective 1. The final model can be seen in Fig. 4.6.

4.10. Summary

This chapter developed a radar range model that is capable of determining the range performance of a radar by calculating the SNR of the reflected signals. It takes into account the power reflected from a target, the noise in the system, clutter in the area, RCS fluctuation, losses in the system and processing gains. From Fig. 4.6 it is clear that the system should be able to detect vehicles at 200 m.

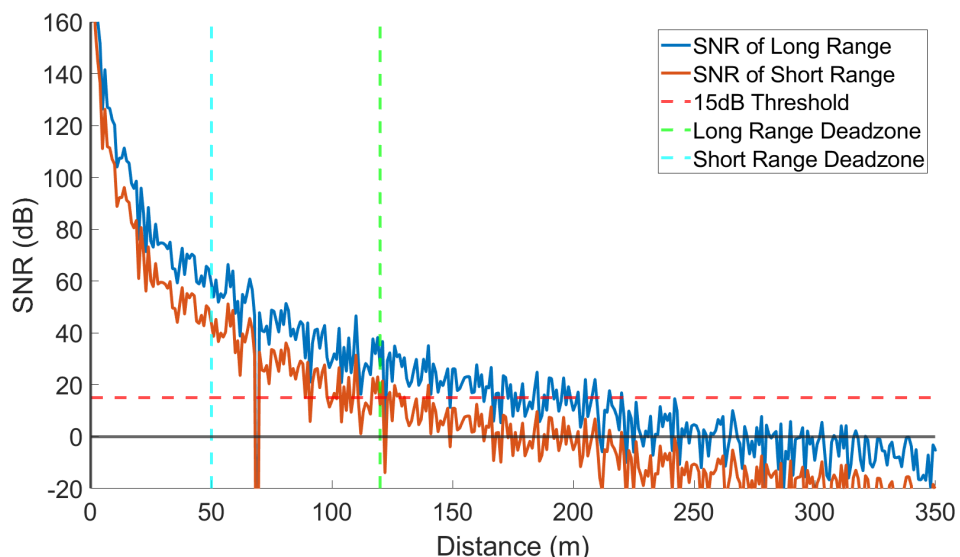


Figure 4.6: Radar detection range model with RCS fluctuation.

Chapter 5

System Implementation

This chapter discusses the process of implementing the system's software and hardware. This includes aspects such as the transmission and reception of the pulses, the data interface, the processing and the display.

5.1. Transmission

For the radar to be able to transmit the pulse, data has to proceed from the host to the antenna. The signal starts as a baseband digital signal and is then processed and modulated onto an analogue carrier. The structure for how this is achieved can be seen in Fig. 5.1.

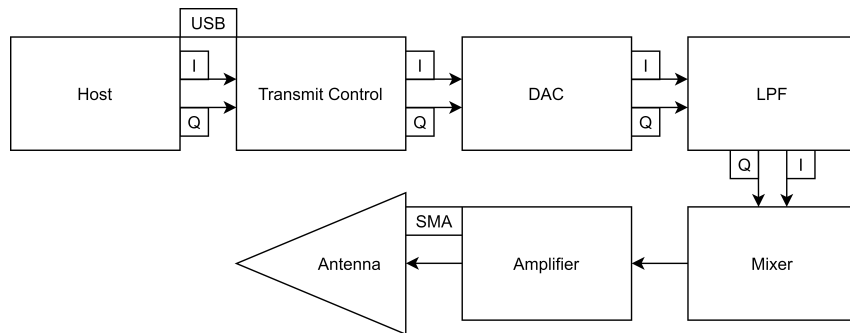


Figure 5.1: The transmission block diagram of the system.

5.1.1. Block Diagram

The signal's I and Q samples (as seen in Fig. 5.5) are sent to the SDR via the USB connection and processed by the transmit controller. It is then converted from a digital signal to an analogue signal via the Digital-to-Analogue Converter (DAC) and taken through a low-pass filter. It is then mixed onto the carrier frequency, amplified and transmitted via the antenna.

5.1.2. Sample Rate

The Ettus B210 has a maximum sample rate of 61.44 MSps. However, Ettus does not recommend the use of sample rates higher than 56 MSps [23]. Sample rates were tested

with the host system and the B210, but these high rates could not be achieved without underflow and overflow. The USB controller of the host system could not feed and receive the SDR with data fast enough. A sampling rate of 16 MSps could be achieved without underflow or overflow.

5.1.3. Gain

The Ettus B210 has a total internal gain of 89 dB available. This value has to be tuned to ensure no clipping happens on the transmission signal. From Fig. 5.2 it is clear that there is still clipping taking place at 89 dB and 86 dB. 83 dB and 80 dB has no clipping and 83 dB is chosen.

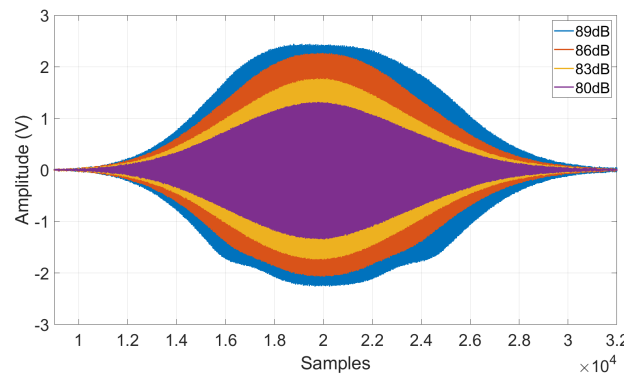


Figure 5.2: Comparison of different gain values for the B210 transmission block.

5.2. Reception

This section discusses how the signals are received from the environment and then processed so that the host can receive the signal as samples. The structure can be seen in Fig. 5.3.

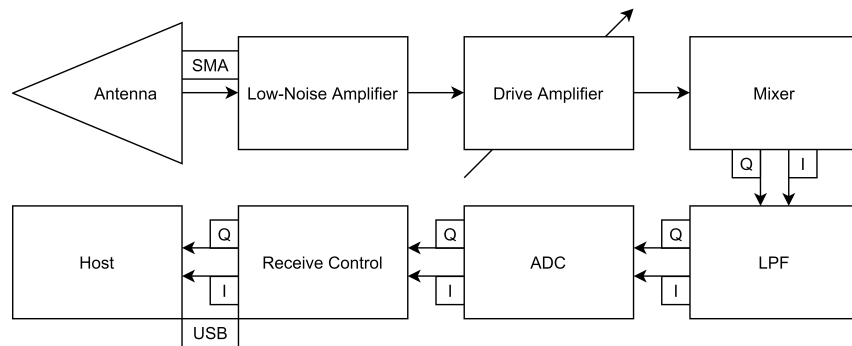


Figure 5.3: The reception block diagram of the system.

5.2.1. Block Diagram

The antenna receives reflections, clutter and noise from the environment. The low noise amplifier then amplifies these low power signals without significantly degrading the SNR

and is then amplified further via the drive amplifier. It is then mixed down to the baseband signal and taken through a low-pass filter. It is then sampled and converted to a digital signal via the Analogue-to-Digital Converter (ADC). It is then processed by the receive controller and the I and Q samples are sent to the host via the USB connection.

5.2.2. Sample Rate

The reception will run at the same rate as the transmission since the B210 does not allow these components to run at separate frequencies.

5.3. Transmission Signal

The signal that is transmitted and received is discussed in this section and the final pulse can be seen in Fig. 5.5.

5.3.1. Transmission Length

When creating a pulsed radar, there is a period when the radar is transmitting the pulse and a period when the radar is receiving the pulse. The longer the pulse is being transmitted, the more energy is illuminating the target, improving the SNR. However, the longer it transmits, the larger the dead zone of the radar becomes. To ensure that the transmitted pulse is perfectly symmetrical, the number of samples in the transmission will be used instead of the time. If 13 and 5 samples are chosen, the dead zones can be calculated as in equations 5.1 to 5.3.

$$t_{\text{TX}} = N_{\text{samples}} \times f_s^{-1} \quad (5.1)$$

$$R_{\text{blind,short}} = \frac{c \times t_{\text{TX,short}}}{2} = 46.84 \text{ m} \quad (5.2)$$

$$R_{\text{blind,long}} = \frac{c \times t_{\text{TX,long}}}{2} = 121.79 \text{ m} \quad (5.3)$$

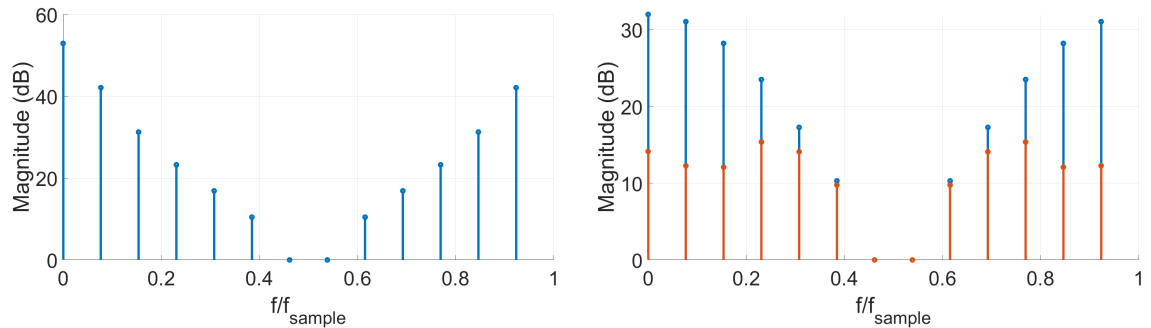
These are the lengths used in the model in Fig. 4.6 and allows the shorter range pulse to compensate for the longer-range pulse. However, as mentioned before, transmission and reception can be used at the same time for this application, but to allow the system to be upgraded later (by adding an amplifier), it will be designed to take dead zones into account.

5.3.2. Frequency Chirp

For the system to be able to increase resolution, pulse compression must be implemented. On the transmission side, there are a few ways to increase the pulse bandwidth for pulse compression. These include linear frequency modulation, non-linear frequency modulation and phase coded signals. A linear chirp method is chosen for simplicity. Since the maximum achievable sampling frequency is 16 MSps, the chirp of the signal must satisfy the condition

$$\Delta f_{\text{chirp}} < \frac{f_s}{2} = 8 \text{ MSps.} \quad (5.4)$$

Taking non-linearities of filters into account, the chirp bandwidth is chosen as 7 MHz. To be able to keep the bandwidth of the signal high and reduce the effects of the sidelobes, a Blackman window is applied. Although the system loses around 3 dB, it can keep the high pulse compression gains from a large bandwidth.



(a) FFT of the transmitted signal with a 1 MHz chirp and without a Blackman window. (b) FFT of the transmitted pulse with a 7 MHz chirp.

Figure 5.4: The effect that windowing has on the maximum bandwidth of signals.

Fig 5.11a shows the bandwidth that was achieved without using a window. A frequency higher than 1 MHz causes aliasing due to large sidelobes. Fig 5.11b shows the aliasing that takes place without a window and the larger bandwidth that is achieved with a window. The increase of the pulse compression gain is calculated by

$$G_{\Delta f} = 10 \log \left(\frac{G_{7\text{MHz}}}{G_{1\text{MHz}}} \right) = 10 \log \left(\frac{t_{\text{TX}} 7}{t_{\text{TX}} 1} \right) = 8.45 \text{ dB} \quad (5.5)$$

where $G_{\Delta f}$ is the gain from the increased chirp bandwidth, $G_{7\text{MHz}}$ is the pulse compression gain at 7 MHz, $G_{1\text{MHz}}$ is the pulse compression gain at 1 MHz and t_{TX} is the transmission time. The net gain from windowing can now be calculated as $8.45 \text{ dB} - 3.29 \text{ dB} = 5.16 \text{ dB}$.

5.3.3. Pulse

All of the parameters discussed above are used to create the transmission signal. Zeros are added so that the radar does not transmit in the time it is receiving. The amount of zeros

required is calculated by

$$N_{\text{zeros}} = \text{ceil}\left(\frac{\text{PRF}^{-1}}{f_s^{-1}}\right) - N_{\text{pulse}} \quad (5.6)$$

where N_{zeros} is the amount of zeros added and N_{pulse} is the amount of samples in the pulse. The final signal can be seen in Fig. 5.5.

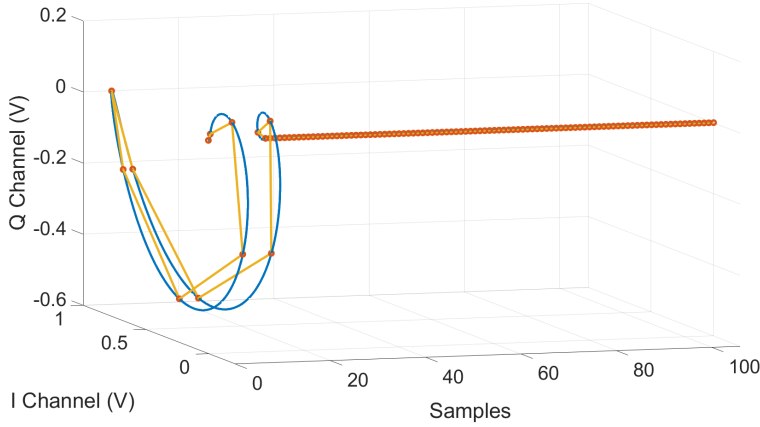


Figure 5.5: The transmission signal pulse with zeros.

5.4. Data Interface

The interface forms a crucial part of the system. It needs to be able to transfer at high data rates and a large number of samples. It is implemented using the UHD C++ API provided by Ettus [13]. Visual Studio [24] was used to develop the C++ interface.

5.4.1. Environment

To set up the UHD environment, the following is required:

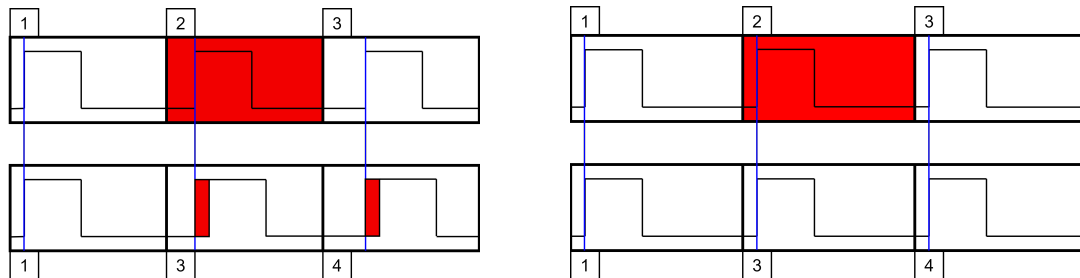
- UHD - As mentioned before, this is the API provided by Ettus that is used to communicate with and control the SDR [13].
- Boost - This contains free libraries for C++ and is required to create threads and format messages [25].
- LibUSB - This is an API that is used by Ettus and required to communicate with their USB devices. [26].

C++ is a language that needs to be compiled. For the code to compile properly, the necessary paths and files from the above-mentioned libraries have to be added to the environment. The following components are required:

- Compilation - Include files (.hpp) and path locations. This includes the files from UHD and Boost.
- Linking - Library files (.lib) and path locations. This includes the files from UHD and Boost.
- Runtime - Dynamic libraries (.dll) locations. This includes the files from UHD, Boost and LibUSB.

5.4.2. Packets

The SDR receives packets from the host. Each of these packets has a maximum size of 2040 samples for the I and Q channel each [13]. Whenever overflow occurs, the SDR discards the current packet and transmits the next packet. The transmission signal that consists of several pulses has to be broken up and can be done in 2 ways. The first method is to take the entire signal and divide it up without taking the individual pulses into account. This leads to a change in the phase when underflow occurs, as seen in Fig. 5.6a. The other method is to place as many full pulses into a packet as possible and ensure that they fit perfectly. This does not lead to a phase change when underflow occurs, as can be seen in Fig. 5.6b.



(a) Packets that cause changes in phase with underflow. **(b)** Packets that do not cause changes in phase with underflow.

Figure 5.6: The effect that packets and underflow has on phase.

5.4.3. Buffers

The buffering on the B210 has three components: transmission streaming ("TX"), reception streaming ("RX") and transferring the received data to the host ("Recv"). The "RX" function receives samples continuously and fills the receive buffer on the SDR. Whenever this buffer is full, the "Recv" function transfers the data to the host and empties the receive buffer on the SDR. On the other hand, "TX" fills the transmit buffer on the SDR with data from the host and then transmits the packet. When the packet has been transmitted, the buffer is emptied and filled with a new packet from the host.

Keeping the transmission and reception synchronized is extremely important. To ensure that the functions that run are not blocked, they each run on a different thread. This can be seen in Fig. 5.7.

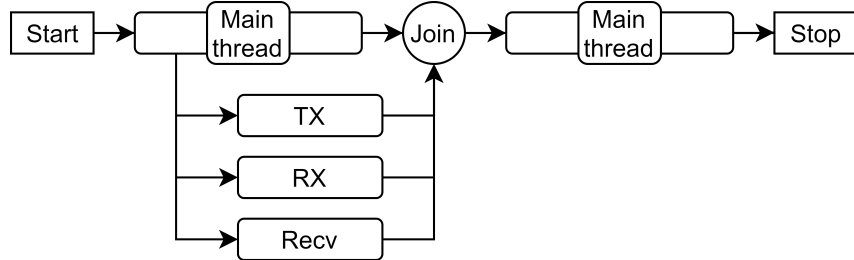


Figure 5.7: The thread diagram for the software in the data interface.

5.5. Processing

This section discusses how the received signals from the SDR are processed to achieve the desired information regarding distance and velocity.

5.5.1. Synchronization

With the B210 it is very difficult to synchronize transmission and reception in hardware. However, there is a way to achieve synchronization in software. When the signal is transmitted via the transmit antenna, it is directly received by the receive antenna. In each pulse, there will be a large peak that is not a return, but the directly transmitted signal. This peak can be used to synchronize the TX and RX. This is done by correlating the received signal with the transmission signal and shifting the largest peak to 0 in range. This is called zero range calibration and can be seen in Fig. 5.8.

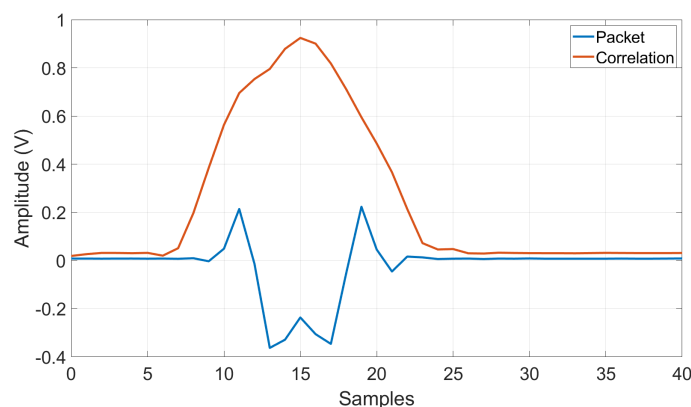


Figure 5.8: Correlation of the packet received by the SDR to synchronize the transmission and reception.

5.5.2. Pulse Compression

To increase the resolution of the system, pulse compression must be implemented and is implemented by using a matched filter. The results from this processing can be seen in Fig. 5.9. The transmitted signal is used instead of a received packet so that the effect can be seen more clearly.

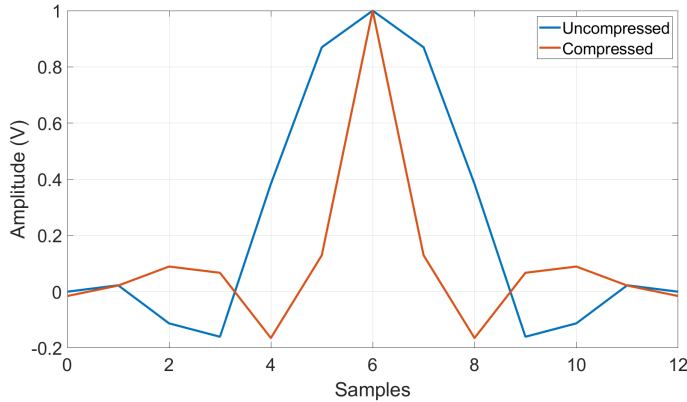


Figure 5.9: The effect of pulse compression on the transmission signal. Both signals are normalised to highlight the effect.

5.5.3. Doppler FFT

A moving target will cause a phase shift in the returned signal, as seen in Fig. 2.5 [7]. This phase shift gives a frequency that can be used to calculate the velocity of the object. The velocity of the target is calculated by

$$V_r = \frac{f_d \times \lambda}{2} = \frac{f_d \times c}{2 \times f_c} \quad (5.7)$$

where f_d is the Doppler frequency and f_c is the carrier frequency. To calculate f_d the return signal is placed in a matrix as seen in Fig. 5.10. The FFT is then calculated over the pulses as shown in Fig. 5.10 and a Blackman window is used to reduce the sidelobes. From section 5.7, 300,000 pulses are used to display, requiring a 2^{19} point FFT. The results from this FFT are displayed to the user. The amplitude of the FFT is encoded in colour.

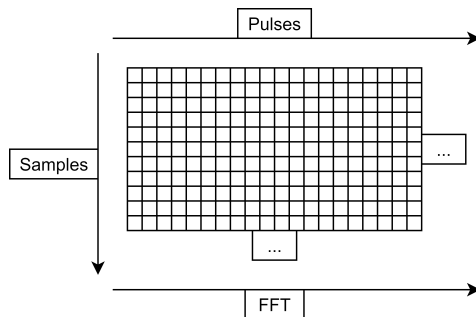


Figure 5.10: The FFT matrix used to calculate the Doppler frequencies.

5.6. Resolution

The system will be limited by the resolution capabilities. There are two types of resolution to be aware of - the resolution at which the radar will be able to detect targets and the resolution at which the radar will be able to display information. Both these are discussed for range and velocity.

The range resolution is determined by two factors, namely the sampling frequency and the width of the signal. If the sampling frequency is higher, finer measurements can be made. The resolution at which the system can display data is calculated by

$$\Delta R = \frac{T_s \times c}{2} = \frac{f_s^{-1} \times c}{2} \approx 9.37 \text{ m} \quad (5.8)$$

where T_s is the sampling period. Pulse compression is used to increase the resolution of the system as seen in Fig. 5.9. If the signal is narrower, peaks can be identified closer to each other. The resolution at which the system can detect targets is calculated by

$$\Delta R = \frac{c}{2 \times B} \approx 21.41 \text{ m} \quad [7] \quad (5.9)$$

where B is the bandwidth of the frequency chirp.

The Doppler/velocity resolution is dependant on the integration time and the number of points used in the FFT. The resolution at which the system can measure targets' speed due to the integration time is calculated by

$$\Delta V_r = \frac{\lambda}{2 \times t_{int}} = \frac{c}{2 \times t_{int} \times f_c} \approx 0.064 \text{ m/s} \quad [7] \quad (5.10)$$

where ΔV_r is the velocity resolution and t_{int} is the integration time. The resolution at which the system can display targets' speed due to the number of points in the FFT is calculated by

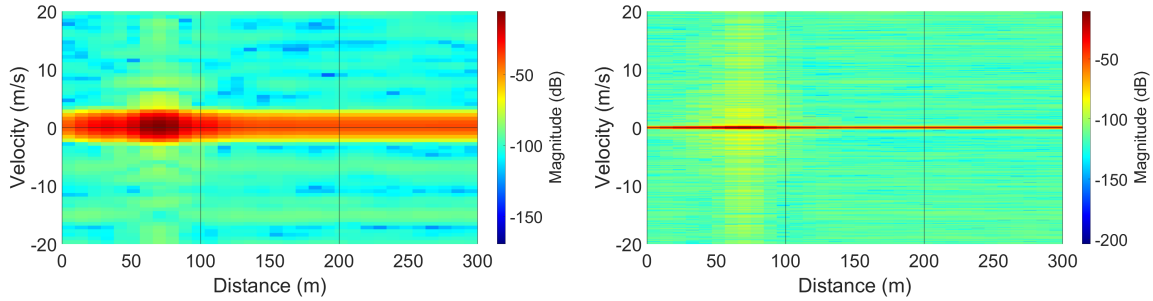
$$\Delta V_r = \frac{0.5 \times \text{PRF}}{N_{FFT}} \times \frac{c}{2 \times f_c} \approx 0.019 \text{ m/s.} \quad (5.11)$$

5.7. Display

This section discusses how the information that is obtained from the processing is displayed in a way that the user can easily read.

C++ is used as the interface between the SDR and the host system and MatLab is used for post-processing since it is easier to use and implement. The data from C++ is written into a file that is read from MatLab. A total of 300,000 pulses ($300,000 \times 107 = 32,100,000$ samples) is written into the file. It is very important to get a high amount of pulses for processing and from Fig. 5.11 it is clear that it leads to an increased resolution. MatLab's

`surf()` [27] function is used to plot the graphs.

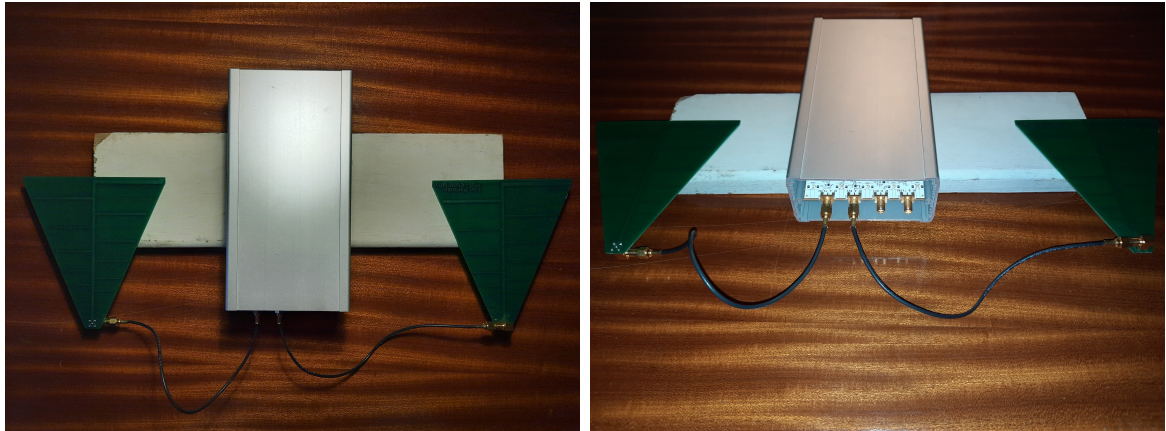


(a) 2^{15} Point Doppler FFT done with 30,000 (b) 2^{19} Point Doppler FFT done with 300,000 pulses.

Figure 5.11: The effect that the amount of pulses used in the Doppler FFT has on the velocity resolution. The received pulse was delayed to highlight the effect of the changes.

5.8. Mounting

The physical implemented system can be seen in Fig. 5.12. The antennas are placed far from each other to minimise coupling. The radar's dimensions are $200 \text{ mm} \times 75 \text{ mm} \times 520 \text{ mm}$.



(a) Top view of the radar.

(b) Front view of the radar.

Figure 5.12: Mounting of the SDR and the antennas onto a plank of wood.

5.9. Summary

This section discussed the practical implementation of the system. It is capable of displaying information at a fine velocity resolution, but the range resolution is still coarse. This can be improved by using a host that is capable of higher sampling frequencies. From Fig. 5.12 it is clear that the system is small enough to be carried by one person, satisfying objective 2. The system does need some changes if an amplifier is to be added, due to the way synchronization is set up. It therefore does not fully satisfy objective 3.

Chapter 6

Radar Performance

6.1. Basic Operation

This section verifies that the most basic components of the radar are functioning as expected before more complex tests are done. Fig. 6.1 shows the results from these measurements.

From Fig. 6.1a the PRF for each of the set of pulses can be calculated as $(13.4927 \mu\text{s} - 6.80357 \mu\text{s})^{-1} = 149.496 \text{ kHz}$ and $(20.1773 \mu\text{s} - 13.4927 \mu\text{s})^{-1} = 149.597 \text{ kHz}$. This is 0.27% from the desired 150 kHz. From Fig. 6.1b the pulse length can be calculated as $7.22595 \mu\text{s} - 6.40291 \mu\text{s} = 823.0 \text{ ns}$. This is 1.29% from the desired 812.5 ns. From Fig. 6.1c the total transmission time can be calculated as $1.17497 \text{ s} + 0.827962 \text{ s} = 2.003 \text{ s}$. This is 0.15% from the desired 2 s. From Fig. 6.1d it is clear that the transmitted signal has a carrier frequency of 1.17 GHz, as per the design. The basic operation of the system is therefore within specification and testing on target detection can now be done.

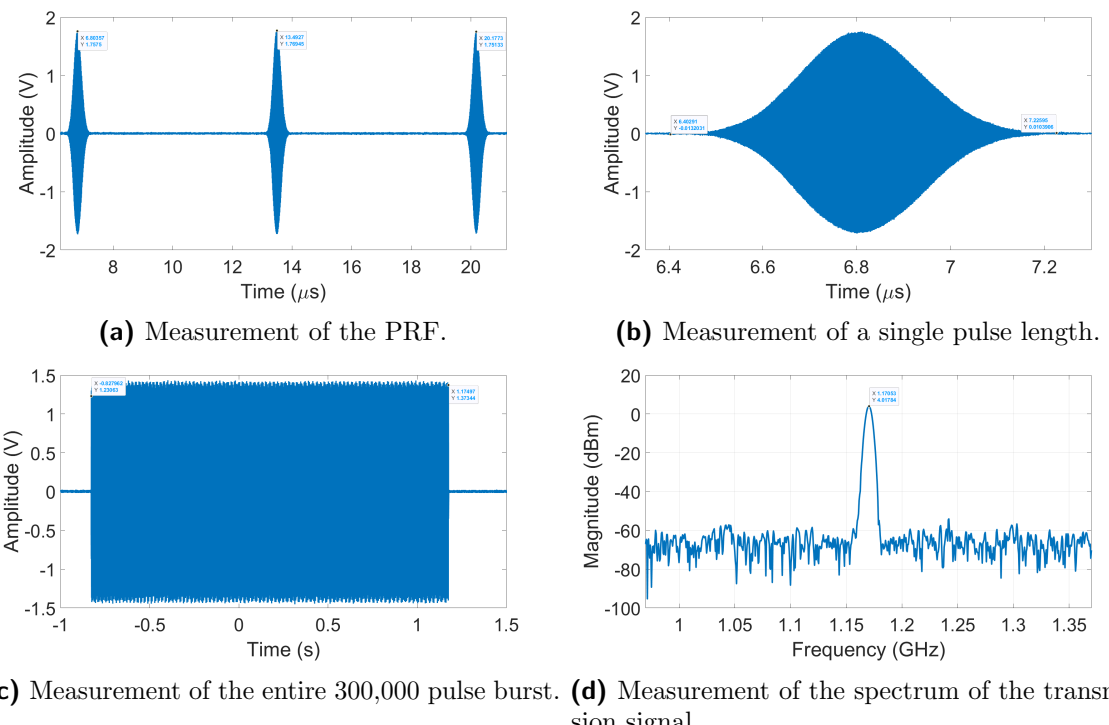


Figure 6.1: Measurements verifying the basic operation of the radar.

6.2. Target Detection

This section discusses the practical test. Fig. 6.2 shows the road where the radar was tested. It is longer than 200 m so that there is room for the vehicles to travel at higher speeds. From Fig. 6.3 it is clear that 2 vehicles are being detected. There are long lines because the transmission time is 2 s and this allows the vehicles to travel roughly 30 m.



Figure 6.2: The road where the radar was tested.

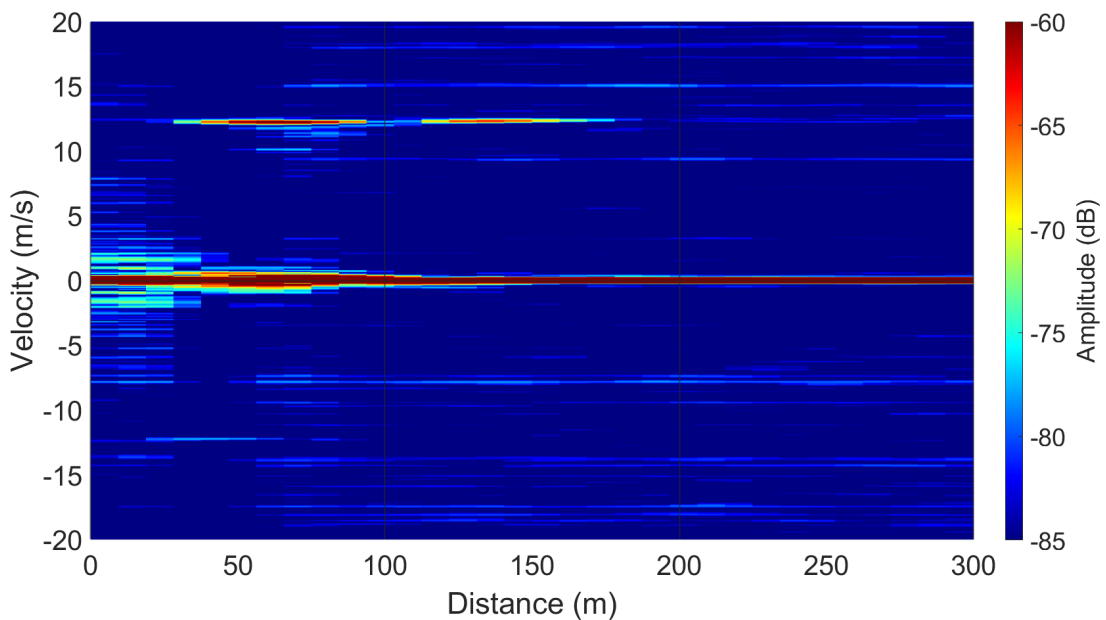


Figure 6.3: Radar detecting two vehicles, one at 65 m and another at 150 m.

Fig. 6.4 shows how a target can be detected using the Doppler effect, even if the clutter has a larger amplitude. The SNR was calculated in Fig. 2.20 by taking the average of each Doppler cell and dividing the entire cell by that value. This reveals a possible third target (or false alarm) at 40 m in the negative velocity region. It is also possible to see

the signal that is received directly from the transmit antenna, at 0 m and 0 m/s. From the calculated SNR values the radar is performing as expected, satisfying objective 1.

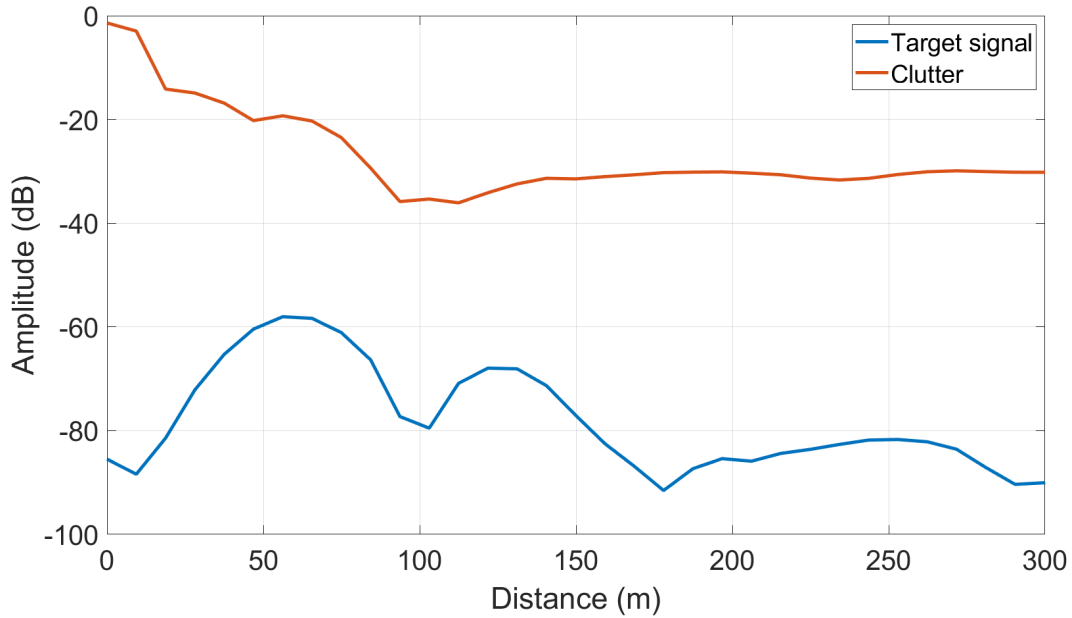


Figure 6.4: Detection of targets even though the clutter's amplitude is higher than that of the targets. The clutter is at a velocity of 0 m/s and the targets at a velocity of 12.24 m/s.

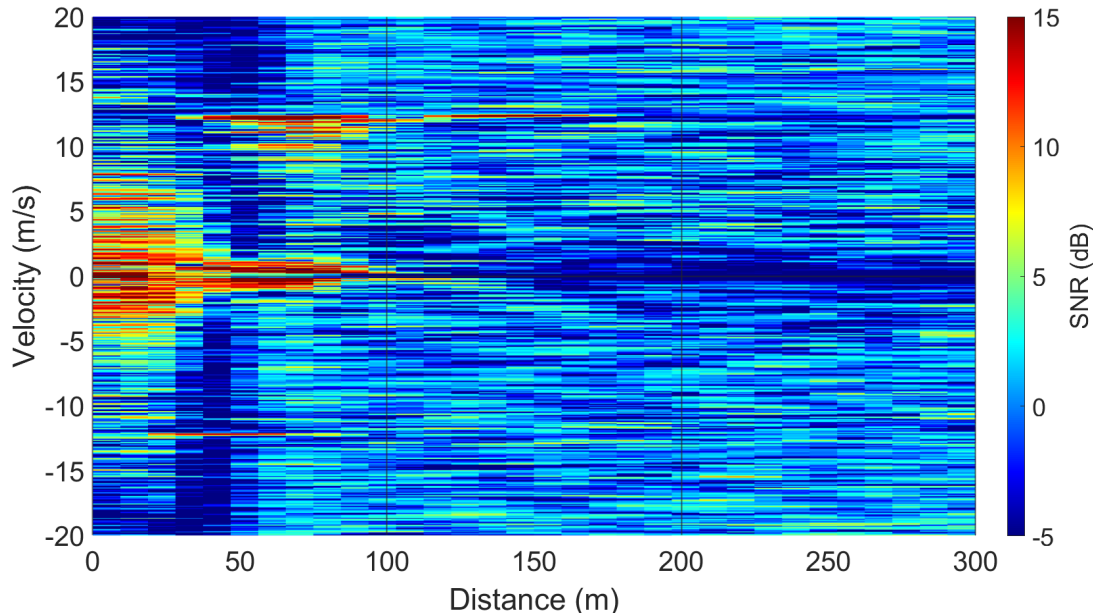


Figure 6.5: The radar detecting targets in the road by calculating the SNR instead of using the amplitude.

Chapter 7

Conclusion

7.1. Summary

This project investigated the design and capabilities of an SDR based pulse-Doppler radar. Before this could be built and implemented there had to be a model to compare the results to. A statistical model of the radar range equation was created and included various elements such as the power received from a target, the noise in the system, clutter, RCS variation, losses and processing gains. From Fig. 4.6 the system should be able to detect targets at 200 m, which satisfies objective 1.

The radar was then implemented using an Ettus B210 SDR and two Ettus LP0965 antennas operating at 1.17 GHz. From Fig. 5.12 it is clear that the system is small enough to be carried by one person, satisfying objective 2. From Fig. 6.3 it is clear that the radar is capable of detecting vehicles at 200 m, satisfying objective 1. The radar can be upgraded with an antenna and only one aspect has to be changed, the synchronization. Therefore, it partially satisfies objective 3.

7.2. Future Work

The field of radar has endless possibilities and the system can be improved in various ways. However, there are a few that are short term.

The first of these is getting the radar to work in real-time. Currently, the system receives the data via C++ and then writes it to a file so that MatLab can execute the post-processing and this process takes too long. The first step in implementing real-time operation would be to implement the post-processing in C++ since this eliminates the use of files and C++ is faster than MatLab. Real-time signal processing algorithms can be implemented in addition to this.

Secondly, the possibility of foliage penetration should be investigated. This concept is briefly touched upon in the report but is not expanded upon. This requires antennas that are capable of transmitting at lower frequencies and thorough testing, which was beyond the scope of this project.

Thirdly, an amplifier can be implemented to enable the radar to detect targets at

longer distances. This will require a new method of synchronization since the radar will not be able to transmit and receive at the same time.

Lastly, the radar can be calibrated using a known RCS target such as a sphere or a trihedral corner reflector. This will allow for RCS measurements of targets and clutter of interest.

Bibliography

- [1] J. KNIGHT. Balloon Reconnaissance, History. encyclopedia.com. [Online]. Available: <https://www.encyclopedia.com/politics/encyclopedias-almanacs-transcripts-and-maps/balloon-reconnaissance-history>
- [2] M. I. Skolnik. History Of Radar. Britannica. [Online]. Available: <https://www.britannica.com/technology/radar/History-of-radar>
- [3] S. Heunis, Y. Paichard, and M. Inggs, “Passive radar using a software-defined radio platform and opensource software tools,” in *2011 IEEE RadarCon (RADAR)*, 2011, pp. 879–884.
- [4] F. Peyrin and J. Friedt, “Study of the use of a sdr passive radar for the safe outdoor operation of an atmospheric lidar,” 03 2019.
- [5] R. Gonçalves Licursi de Mello, F. Sousa, and C. Junqueira, “Sdr-based radar-detectors embedded on tablet devices,” 08 2017, pp. 1–5.
- [6] C. Wolff. Radar Cross-Section. radartutorial.eu. [Online]. Available: <https://www.radartutorial.eu/01.basics/Radar%20Cross%20Section.en.html>
- [7] C. Alabaster, *Pulse Doppler Radar: Principles, Technology, Applications*, ser. Electromagnetics and Radar. Institution of Engineering and Technology, 2012. [Online]. Available: <https://books.google.co.za/books?id=p7FRyhwDbgMC>
- [8] CSIR Home Page. CSIR. [Online]. Available: <https://www.csir.co.za/>
- [9] RSPdx. SDRplay. [Online]. Available: <https://www.sdrplay.com/rspdx/>
- [10] SDRplay, *RSPdx Multi-antenna port 14-bit SDR*, Jun 2020, version 1.3.
- [11] USRP B210. Ettus Research. [Online]. Available: <https://www.ettus.com/all-products/ub210-kit/>
- [12] Nuand BladeRF 2.0 micro. Nuand. [Online]. Available: <https://www.nuand.com/bladerf-2-0-micro/>
- [13] API Documentation. Ettus. [Online]. Available: https://files.ettus.com/manual/page_uhd.html

- [14] Products Antennas. Ettus Research. [Online]. Available: <https://www.ettus.com/product-categories/antennas/>
- [15] Home Page. GNU Radio. [Online]. Available: <https://www.gnuradio.org/>
- [16] USRP Support from Communications Toolbox. MatLab. [Online]. Available: <https://www.mathworks.com/hardware-support/usrp.html>
- [17] B200/B210/B200mini/B205mini. Ettus Research. [Online]. Available: <https://kb.ettus.com/B200/B210/B200mini/B205mini>
- [18] LP0965 Antenna. Ettus Research. [Online]. Available: <https://www.ettus.com/all-products/lp0965/>
- [19] “Government gazette - staatskoerant,” REPUBLIC OF SOUTH AFRICA - REPUBLIEK VAN SUID AFRIKA, May 2018, vol. 635, no. 41650, ISSN 1682-5843.
- [20] H. M. Rahim, C. Y. Leow, and T. A. Rahman, “Millimeter wave propagation through foliage: Comparison of models,” in *2015 IEEE 12th Malaysia International Conference on Communications (MICC)*, 2015, pp. 236–240.
- [21] F. J. Harris, “On the use of windows for harmonic analysis with the discrete fourier transform,” *Proceedings of the IEEE*, vol. 66, no. 1, pp. 51–83, 1978.
- [22] C. Wolff. Typical Search Radar Loss Budget. radartutorial.eu. [Online]. Available: <https://www.radartutorial.eu/01.basics/Typical%20Search%20Radar%20Loss%20Budget.en.html#:~:text=These%20are%20losses%20due%20to,Gigahertz%20by%20clear%20weather%20conditions>
- [23] Comparative features list - B200/B210/B200mini. Ettus. [Online]. Available: https://files.ettus.com/manual/page_usrp_b200.html
- [24] Visual Studio - Best-in-class tools for any developer. Microsoft. [Online]. Available: <https://visualstudio.microsoft.com/>
- [25] R. R. Beman Dawes, David Abrahams. Boost C++ Libraries. [Online]. Available: <https://www.boost.org/>
- [26] libusb - A cross-platform user library to access USB devices. libusb. [Online]. Available: <https://libusb.info/>
- [27] surf - Surface plot. MatLab. [Online]. Available: <https://www.mathworks.com/help/matlab/ref/surf.html>

Appendix A

Project Planning Schedule

Table A.1: Project planning schedule.

Week start	Work planned
29/06/2020	Skripsie starts.
29/06/2020	Study textbook (Pulse Doppler Radar Principles, Clive Alabaster).
05/07/2020	Study textbook (Radar Handbook, Merril Skolnik).
12/07/2020	Study papers provided by CSIR.
19/07/2020	Study and derive the radar range equation.
26/07/2020	Implement the radar range equation in MatLab.
02/08/2020	Compare hardware and software options. Implement the MatLab interface.
09/08/2020	Test the MatLab interface. Make antenna measurements. Learn C++.
16/08/2020	Set up the C++ environment and data interface with the SDR. Learn the UHD API.
23/08/2020	Set up transmission and reception on the SDR. Create a MatLab model of the transmission.
30/08/2020	Synchronize transmission and reception on the SDR.
07/09/2020	Implement post processing and displaying in MatLab. Set up communication between C++ and MatLab.
14/09/2020	Implement post processing in C++. Create FEKO model of RCS.
21/09/2020	Refine and optimize code.
28/09/2020	Run tests on radar.
04/10/2020	Write report.
11/10/2020	Write report.
18/10/2020	Write report.
25/10/2020	Write report and hand in for review.
02/11/2020	Refine report.
09/11/2020	Skripsie deadline.

Appendix B

Exit Level Outcomes

Table B.1: Exit level outcomes: descriptions and chapters.

ELO	Description	Chapters
1	Problem solving: Identify, formulate, analyse and solve complex engineering problems creatively and innovatively.	1, 4, 5.
2	Application of scientific and engineering knowledge: Apply knowledge of mathematics, natural sciences, engineering fundamentals and an engineering speciality to solve complex engineering problems.	2, 4, 5.
3	Engineering Design: Perform creative, procedural and non-procedural design and synthesis of components, systems, engineering works, products or processes.	3, 4, 5.
4	Investigations, experiments and data analysis: Demonstrate competence to design and conduct investigations and experiments.	3, 4, 5, 6.
5	Engineering methods, skills and tools, including Information Technology: Demonstrate competence to use appropriate engineering methods, skills and tools, including those based on information technology.	4, 5.
6	Professional and technical communication: Demonstrate competence to communicate effectively, both orally and in writing, with engineering audiences and the community at large.	All.
8	Individual work: Demonstrate competence to work effectively as an individual.	All.
9	Independent Learning Ability: Demonstrate competence to engage in independent learning through well-developed learning skills.	All.

Table B.2: Exit level outcomes: motivations.

ELO	Motivation
1	A complex problem was presented and to be able to successfully provide a solution it had to be broken down into various smaller problems. This included mathematical problems that arose with the understanding of radar theory and post-processing algorithms, problems with hardware that required debugging with measurement tools and an understanding of low-level electronics, problems in software that required creative use of buffers, objects, variables, etc. and problems that arose with the writing, reading, processing and displaying of data and information.
2	Before the radar could be built a proper understanding of radar systems and theory had to be acquired. This lead to an extensive period spent studying textbooks and papers. This included topics such as electromagnetic wave theory, telecommunications theory, the Doppler effect and post-processing algorithms, to name a few.
3	This project included the design of an algorithm that predicts the performance of a radar, as well as the building, designing and implementation of a radar. It, therefore, consists of both software and hardware engineering design. It also required an extensive mathematical analysis of the radar range equation to ensure the optimum SNR is achieved by choosing the correct parameters.
4	Thorough investigations were done regarding the choice of the hardware, software and the parameters of the radar. An algorithm was developed to investigate the effect of parameters on radar performance. The software was tested to see how well it performs. Antennas were measured to see which frequencies provide the best performance. FEKO models were used to estimate RCS values.
5	This project involved the measuring of antennas and signals using an oscilloscope, a network analyzer and an anechoic chamber. It also involved the use of software tools such as FEKO, MatLab, the UHD API and setting up a C++ environment. Engineering design and project management methods were also used.
6	Weekly meetings were held with the supervisor and some meetings were held with the CSIR to discuss the progress of the project. These meetings were very similar to meetings that are held in the engineering profession. The outcome is also met by the writing of a technical report and presenting the project to qualified engineers.
8	This project was completed by my decisions, planning and execution. External input was only via meetings for high-level guidance and some guidance on very difficult problems or theory.
9	This project required the learning of telecommunications and radar theory since robotics was chosen as an undergraduate study stream. Various textbooks and papers had to be studied and the theory learnt had to be implemented to build a functioning radar.